SOLAR ENERGY TECHNOLOGIES OFFICE
U.S. Department Of Energy

Characterization of Convective and Particle Losses in High-Temperature Particle Receivers

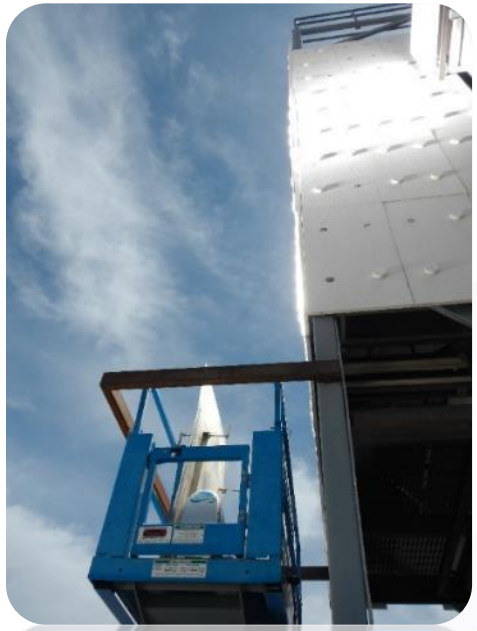

Phase/Quarter: BP2, Q7

Presentation date: 2/5/21

DOE Phase Funding: $631,496 (BP1), $399,574 (BP2)

Principal Investigator: Clifford K. Ho

Other Contributors: SNL (Andres Sanchez, Andrew Glen, Darielle Dexheimer), University of New Mexico (Jesus Ortega, Peter Vorobieff, Gowtham Mohan)

Sandia National Laboratories

Award CPS #33869

Problem Statement

- Particles can escape from the open aperture of a falling particle receiver
  - Inhalation/pollution hazard
  - Loss of particle inventory
- Need to minimize both particle *and* convective heat losses
  - Can imaging of particles be used to estimate particle and convective heat losses?

Nov. 2, 2015
3/8” slot – free fall
280 micron ACCUCAST ID50
10-15 mph south wind
500 – 1000 suns

Project Objectives

1. Task 1: Develop imaging methods to characterize particle and heat losses emitted from the aperture of a high-temperature particle receiver
2. Task 2: Quantify particle emissions using standard air monitoring procedures and compare to OSHA and EPA standards

Work Planned for this Quarter

- Task 1: In-situ sensing and imaging methods
  - Improve estimation of particle mass flow rate using IR camera
  - Process data from on-sun testing at NSTTF
- Task 2: Air Monitoring
  - Perform far-field tethered-balloon particle sampling during on-sun tests

- Publish results

Task 1: Particle Imaging (UNM)

Task 1: Particle Imaging (UNM)

- In Q7of BP2, we performed bench-scale tests to validate the mass flow rate estimation methodology against measured mass flow rate
  - The results showed an agreement for the cases that we analyzed based on a correction that we made for the initial velocity reference location
- We began processing imaging of on-sun experiments of the falling particle receiver at Sandia
  - Results showed consistent mass flow rates with previous tests and convective heat losses that were consistent with measured values of receiver efficiency

Plume Mass Flow Rate Extraction Methodology

SOLAR ENERGY TECHNOLOGIES OFFICE
U.S. Department Of Energy

Task 1: Particle Imaging (UNM)

Plume Mass Flow Rate Extraction Methodology

- The mass flow rate is defined as:

$$\dot{m}_b = \rho_b A_c V_b \quad (1)$$

- Where the mass flow rate ($\dot{m}_b$) is a function of the bulk density (ρ_b), the flow (cross-sectional) area, (ρ_b) and the bulk velocity of the particles (V_b).
- The bulk density can then be substituted by the volume fraction relationship:

$$\rho_b = \varphi\, \rho_p \quad (2)$$

- Where (φ) is the particle volume fraction and (ρ_p) is the particle density.
- Finally, the mass flow rate equation can be expanded to:

$$\dot{m}_p = \varphi\, \rho_p\, w_c\, t_c\, V_b \quad (3)$$

- Where the area of the flow is the product of the width (w_c) and thickness (t_c) of the plume

Task 1: Particle Imaging (UNM)

Plume Mass Flow Rate Extraction Methodology

- Applying the Modified Beer's Law Equation presented by Kim et al:

$$\omega = 1 - e^{-\frac{3\varphi t_c}{2d_p}} \quad (4)$$

- Where the opacity (ω) is a function of the particle volume fraction (φ), the plume thickness (t_c) and the particle diameter (d_p).
- Rewriting equation 4 and plugging it into equation 3:

$$\dot{m}_p = -\frac{2}{3} d_p \rho_p w_c V_b ln(1 - \omega) \quad (5)$$

- It should be noted that the opacity is calculated using the imaging methodology presented in the past.

Task 1: Particle Imaging (UNM)

- A sample curtain was generated at UNM with a mass flow rate of 5.2 g/s
  - Using the Nikon images, an opacity profile was developed as a function of discharge position.
  - The bulk velocity was assumed to flow the free-fall velocity profile.

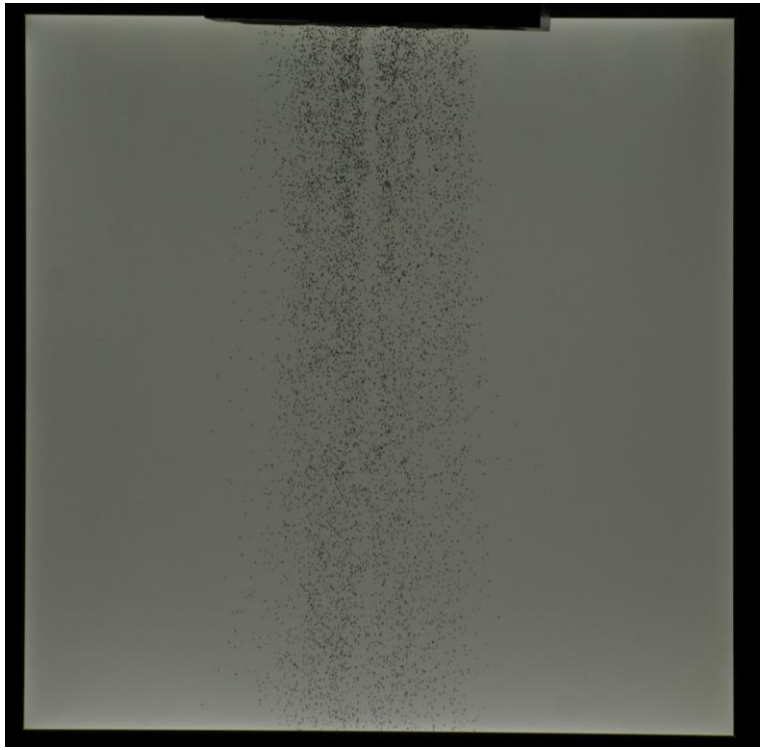

Sample image of a particle curtain with mass flow rate of 5.2 g/s

Task 1: Particle Imaging (UNM)

- A cold-flow sample curtain was generated at UNM with a mass flow rate of 5.2 g/s
  - Using the Nikon images, an opacity profile was developed as a function of discharge position.
  - The bulk velocity was assumed to flow the free-fall velocity profile.
    - No thermograms captured for cold-flow tests
  - However, as seen on the figure, the mass flow rate is underestimated by the correlation
    - This led the team to believe there were some physics incorrectly captured by equation 5

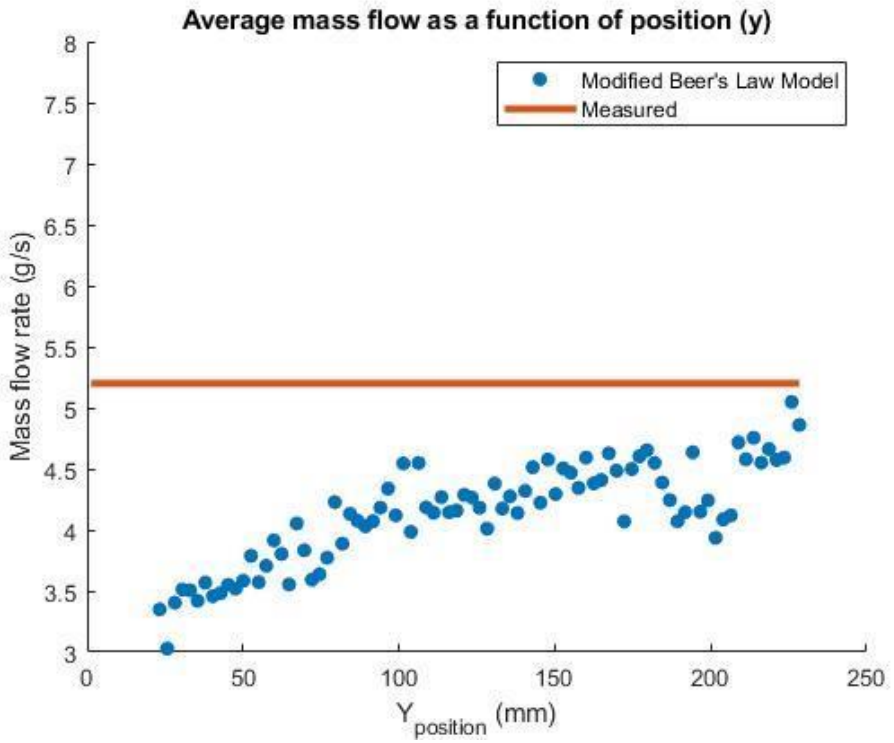

Mass flow profile of a 5.2 g/s curtain

Task 1: Particle Imaging (UNM)

Initial Velocity Reference

- If we were to consider the drop height from nozzle and plate as we take the images at the edge of the nozzle, we will need to add an initial velocity to the velocity profile used in the calculations

$$V = \sqrt{2\ x\ 9.81 \frac{m}{s^2}\ x\ 0.015875m}$$

$$V = 0.5581\ m/s$$

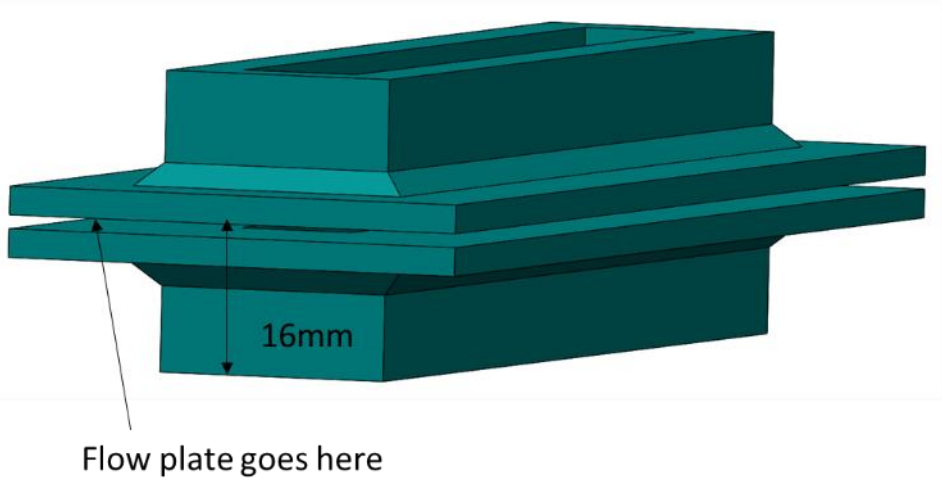

Geometry of flow nozzle used on the top hopper of the SPR at UNM

Task 1: Particle Imaging (UNM)

- A sample curtain was generated at UNM with a mass flow rate of 5.2 g/s
  - If we include the initial velocity calculated for the corrected reference point, as seen on the figure, the mass flow rate estimated agrees with the average measured using the scale.
  - Similarly, the other two cases presented on the quarterly report show that the predicted mass flow rate agrees well with the measured values.

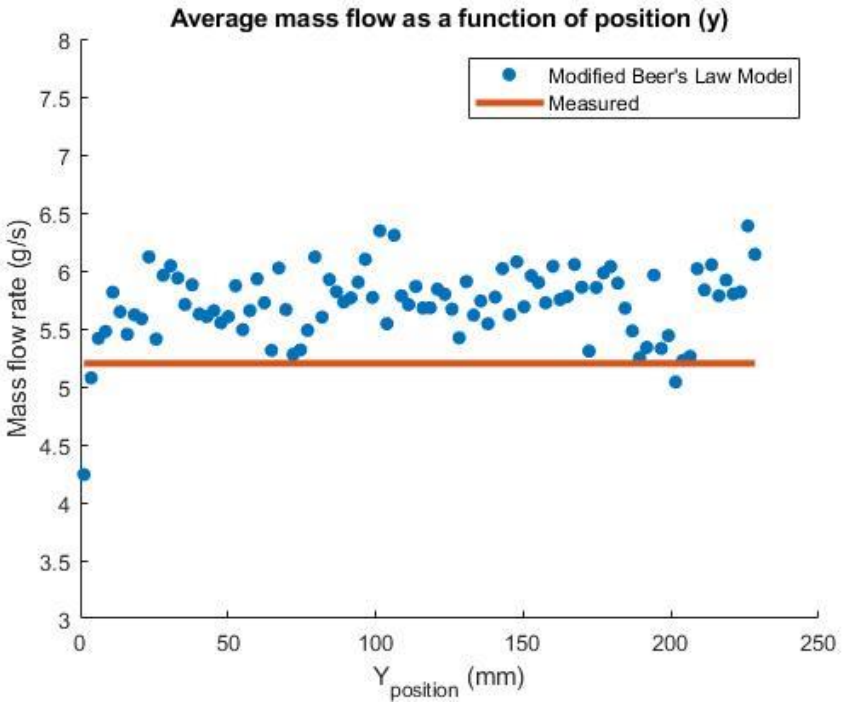

Mass flow profile of a 5.2 g/s curtain with the modified velocity profile

On-Sun Testing Post-processing Results

Task 1: Particle Imaging (UNM)

Focus of this work

- The focus is to post-process on-sun test results
- We have successfully completed the code which will be used to post-process the image sequences

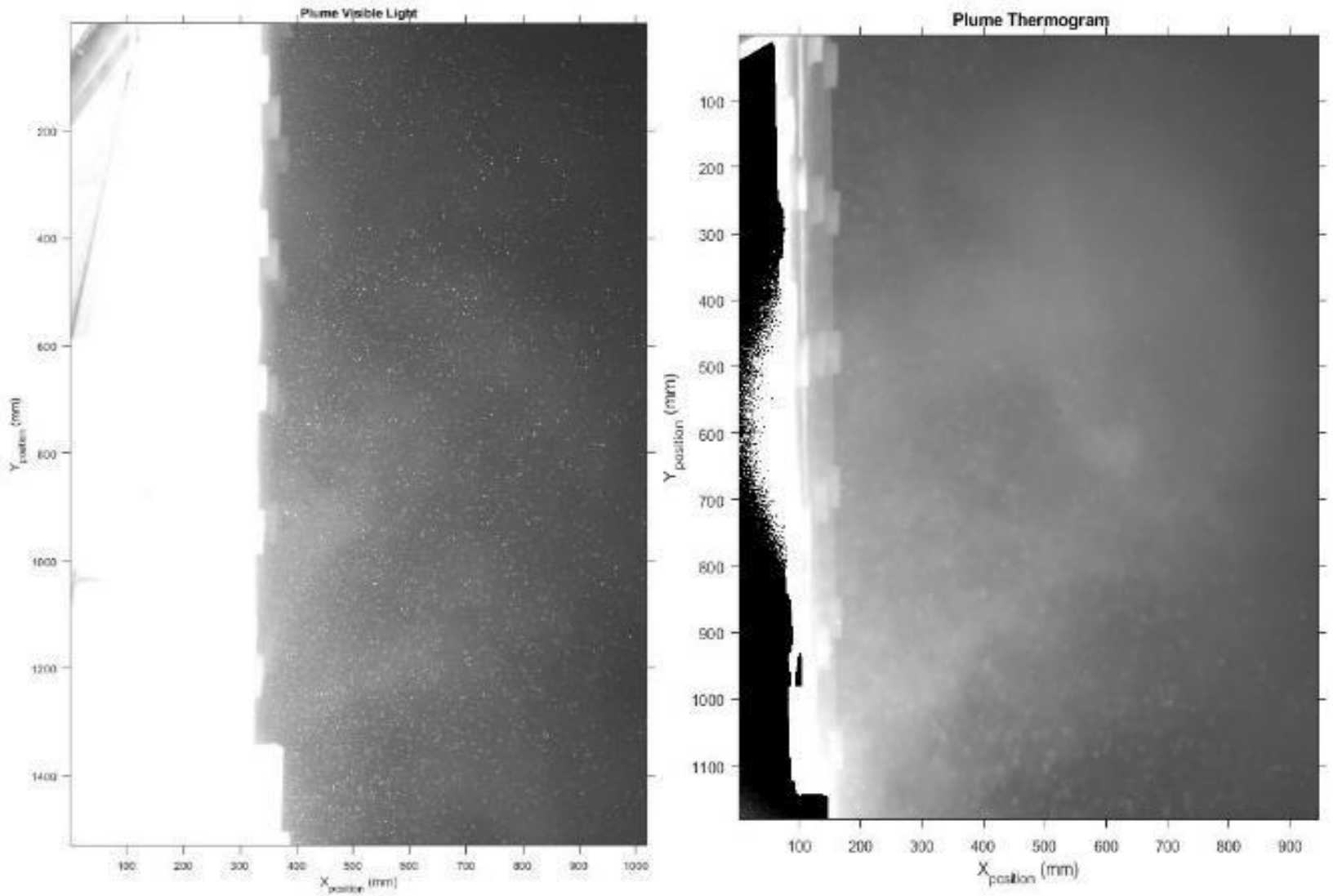

Filtering of Visible-light and Thermograms

SOLAR ENERGY
TECHNOLOGIES OFFICE
U.S. Department Of Energy

Task 1: Particle Imaging (UNM)

Filtering of Nikon Images

- In order to remove the dust in the background and leave the particles only, a median filter was applied to remove outliers.
- The results show that a matrix size of approximately 90x90 converges to a value of 0.9006 which means that the images are approximately 90% similar since the outliers were filtered out.

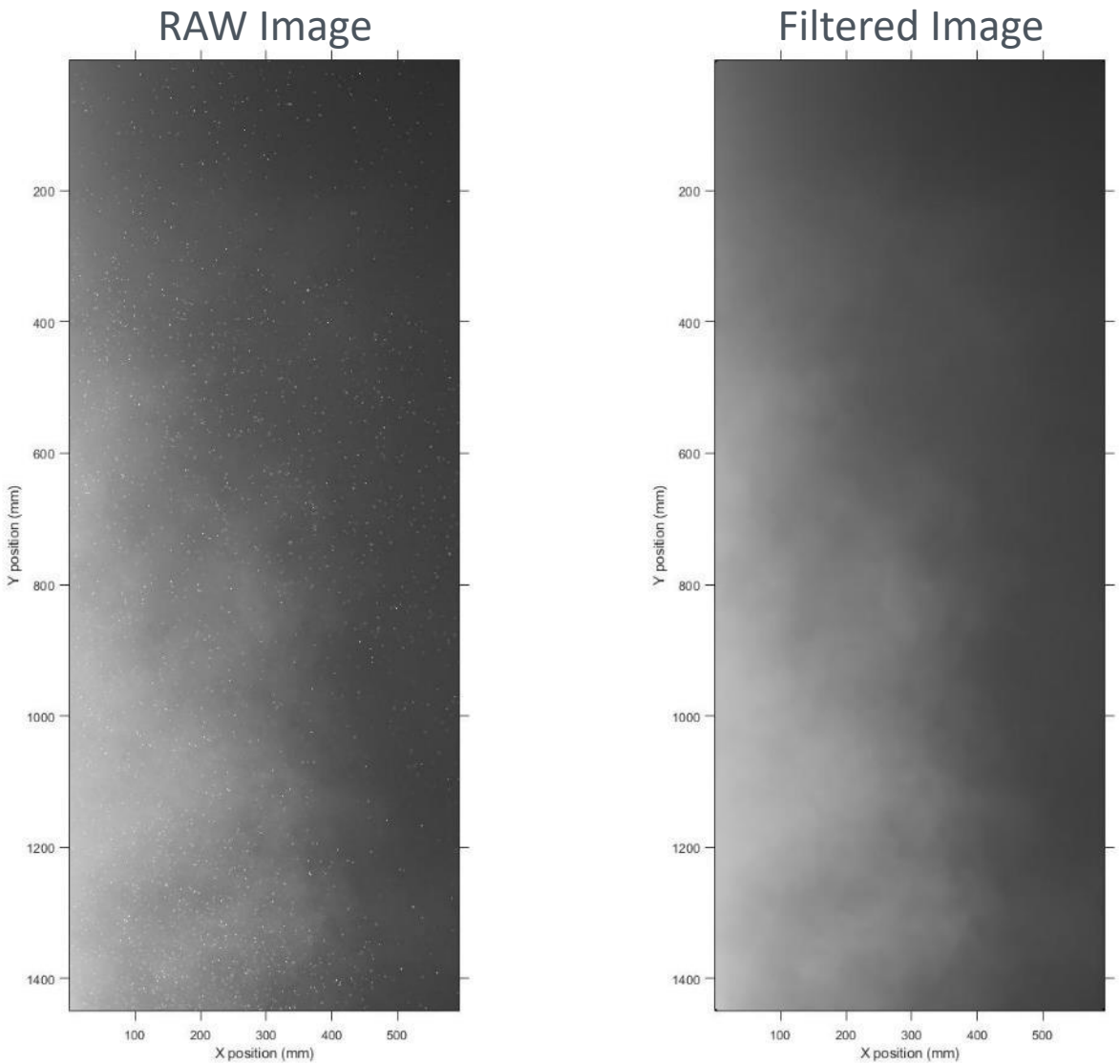

Task 1: Particle Imaging (UNM)

Filtering of Nikon Images

- The structural similarity index measure (SSIM) is a good metric to assess the effect of removing the particles from the RAW image

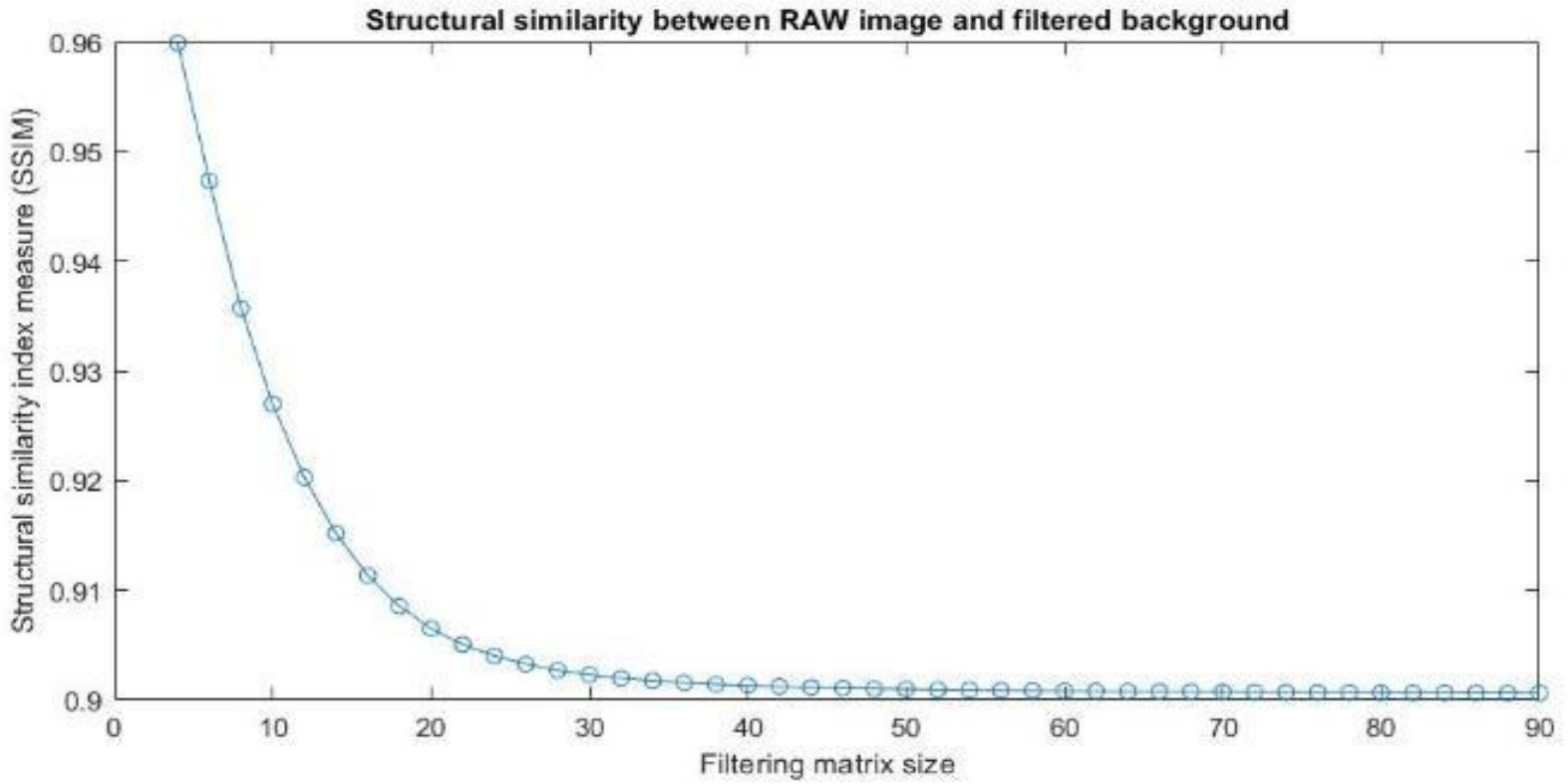

Task 1: Particle Imaging (UNM)

Filtering of Nikon Images

- Once the pixels with outliers (particles) are removed, the code searches for those pixels on the original image to leave an image with particles only

RAW Image

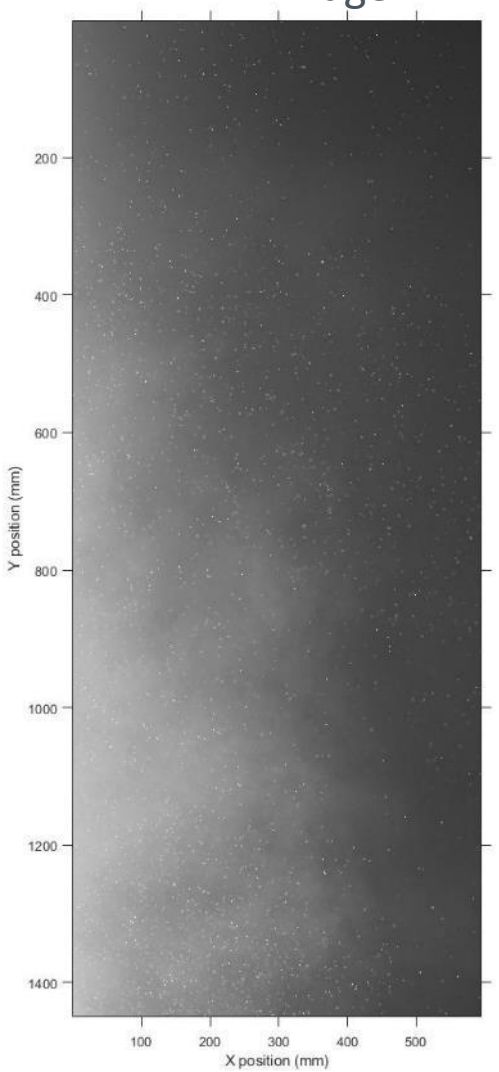

Clean Image

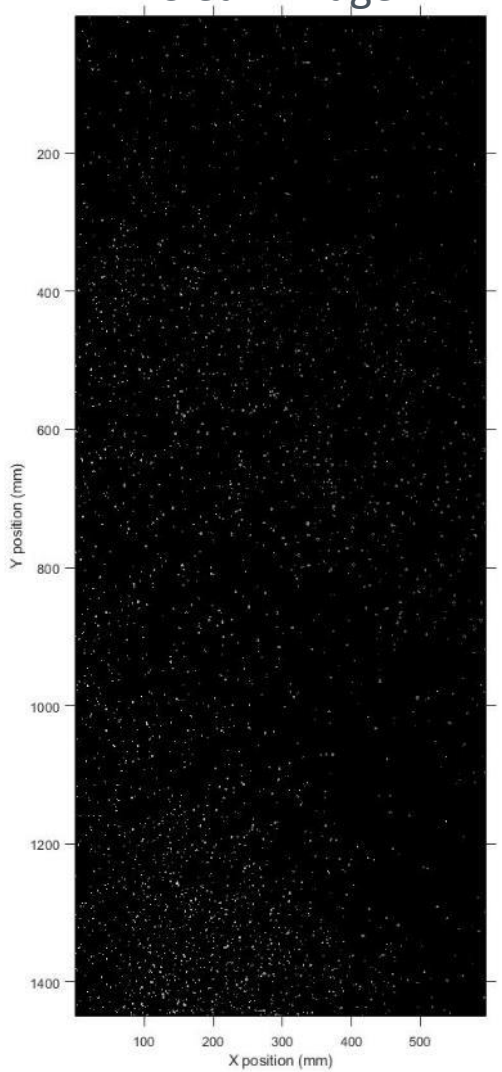

Task 1: Particle Imaging (UNM)

Opacity Calculations

- The opacity calculation generates a profile as shown in the figure.
- This opacity vector generated for every Nikon image is stored in a local database for future calculations.

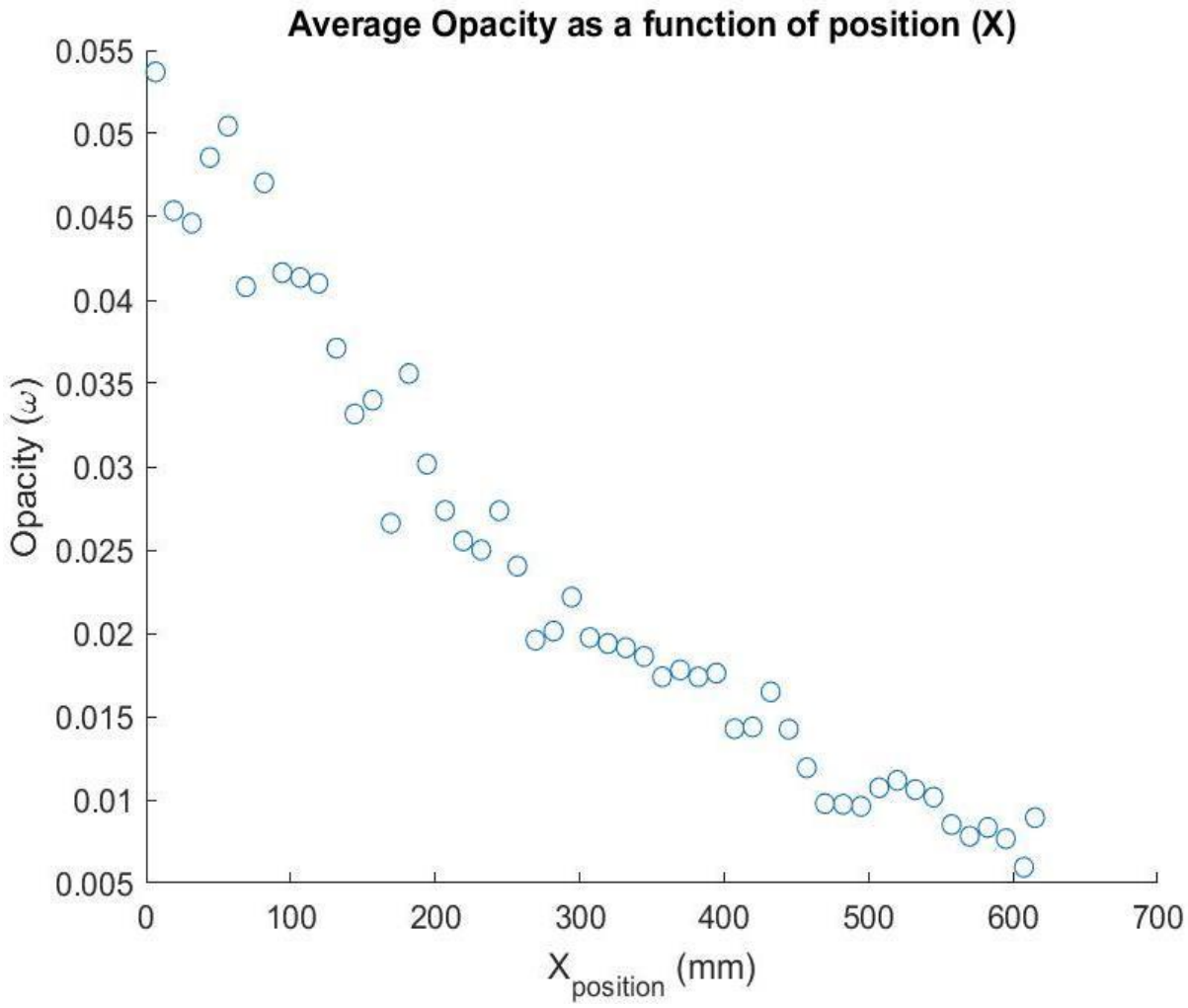

Task 1: Particle Imaging (UNM)

Filtering Thermograms

- The same median filtering routine was applied to remove outliers from thermograms.
- The results show that a matrix size of approximately 25x25 will sufficiently eliminate all the temperature outliers and will yield an image that does not contain particles

RAW Image

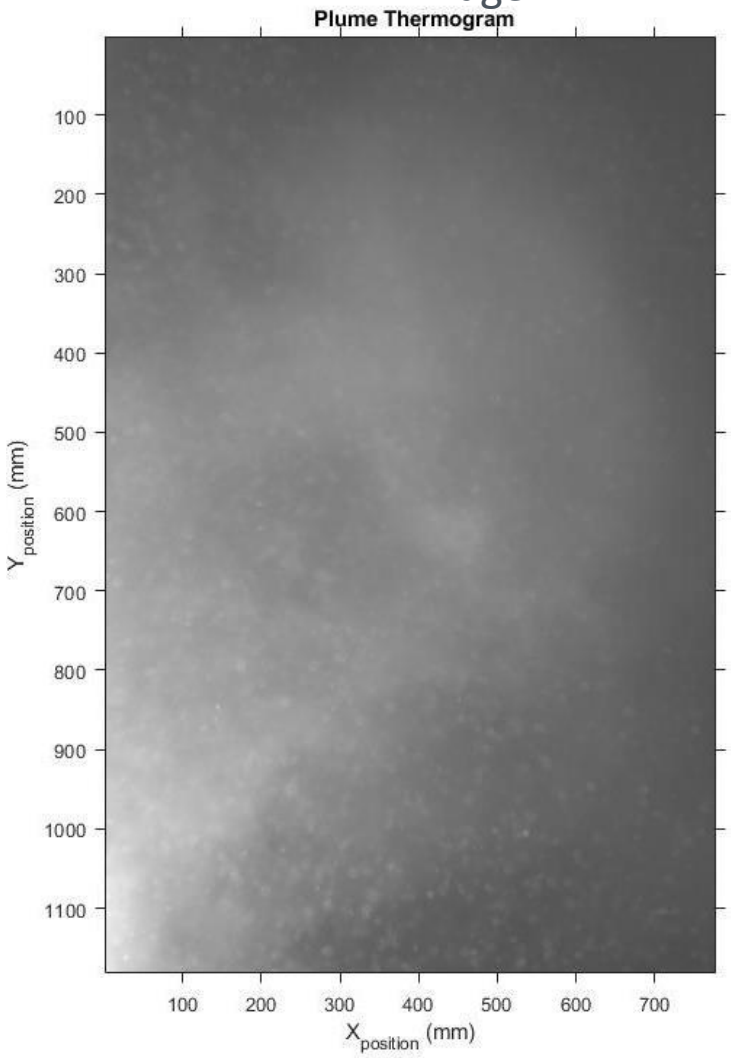

Filtered Image

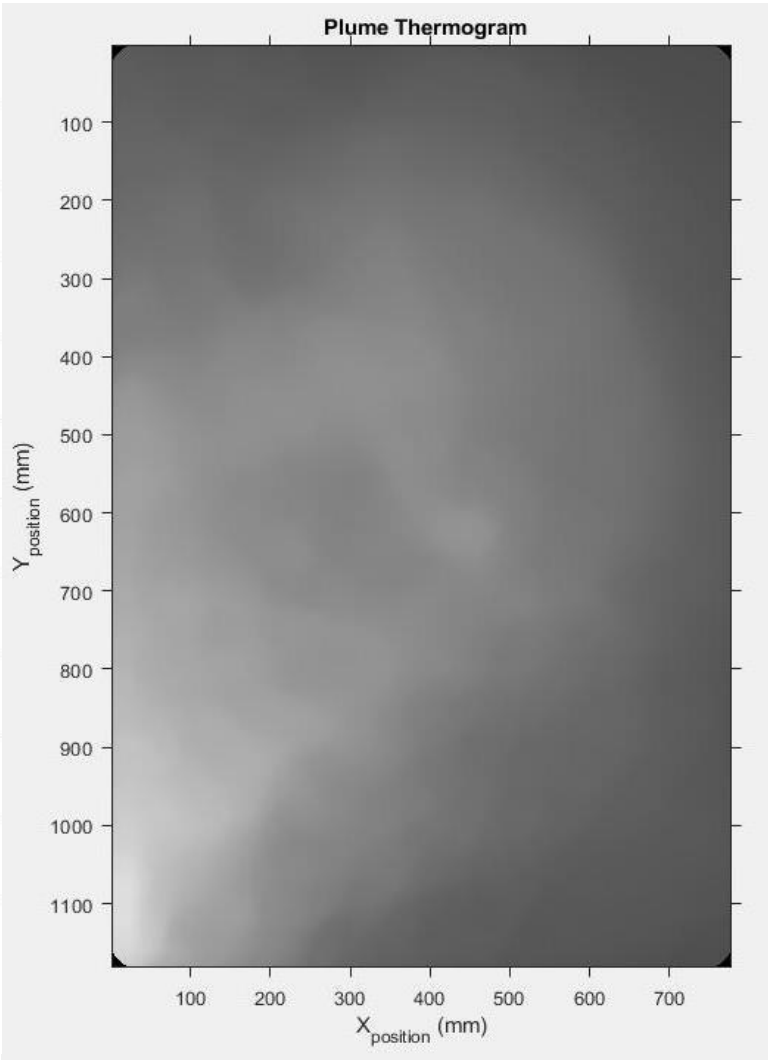

Task 1: Particle Imaging (UNM)

Filtering Thermograms

- Once the pixels with outliers (particles) are removed, the code searches for those pixels on the original image to leave an image with particles only

RAW Image

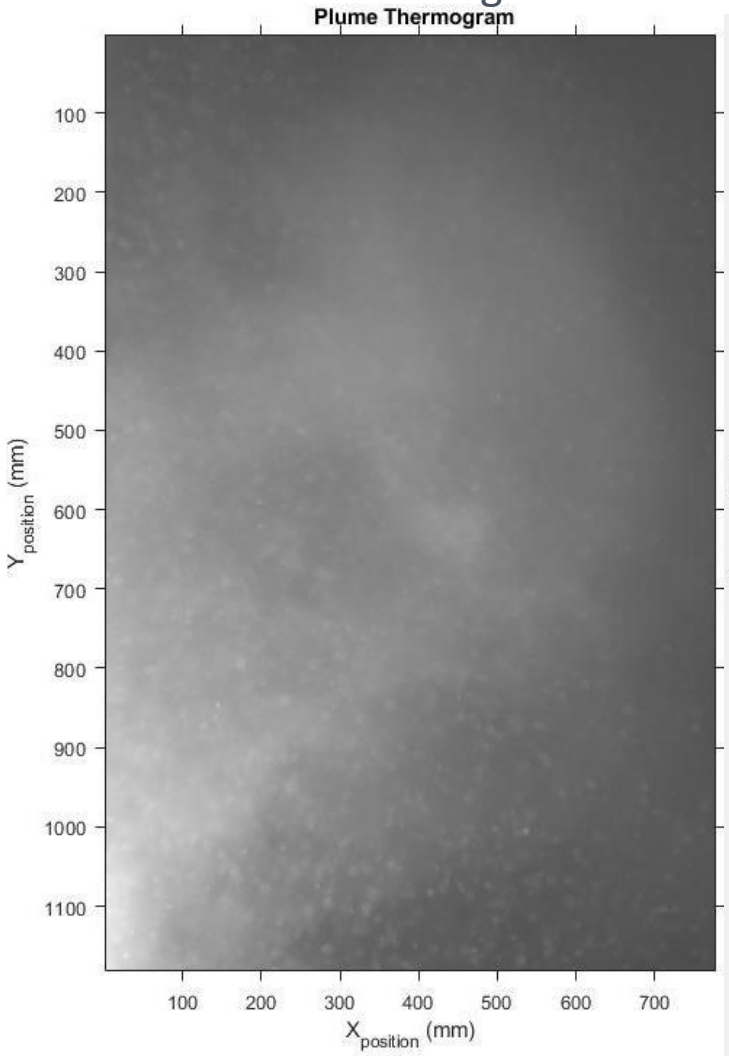

Clean Image

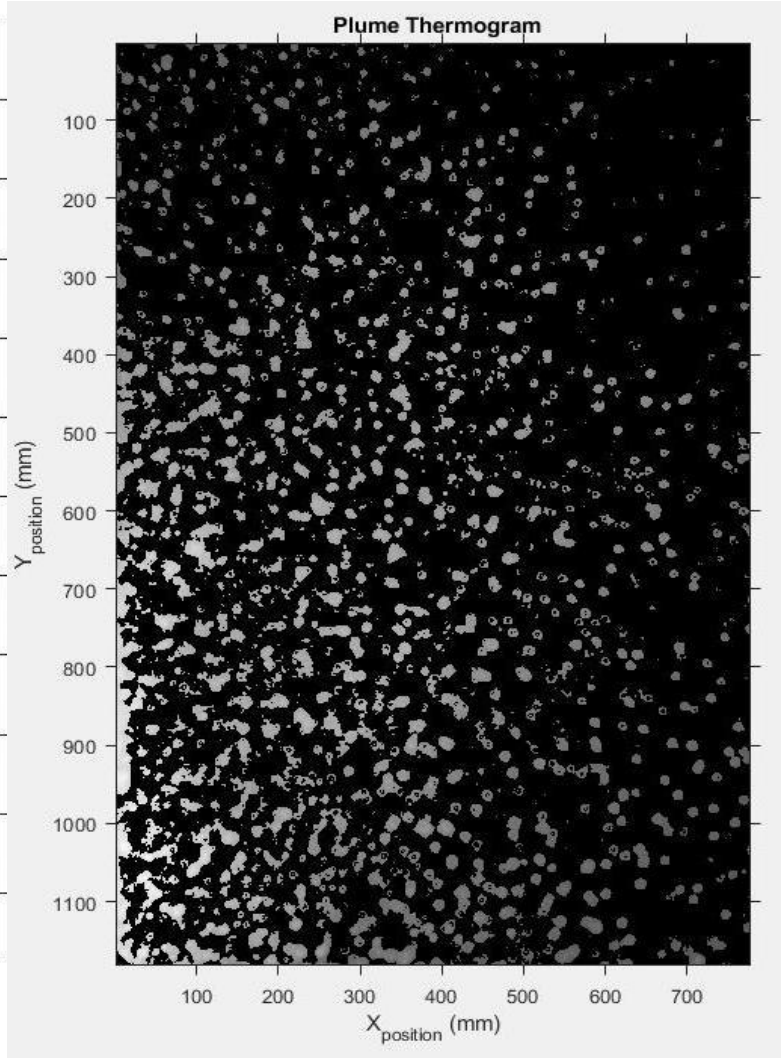

Task 1: Particle Imaging (UNM)

Average Pixel Temperature

- The average pixel temperature profile, as shown in the figure, is generated by averaging the matrices that contain particles only and show temperatures above the background temperature.
- This average pixel temperature vector generated for every thermogram set and it is stored in a local database for future calculations.

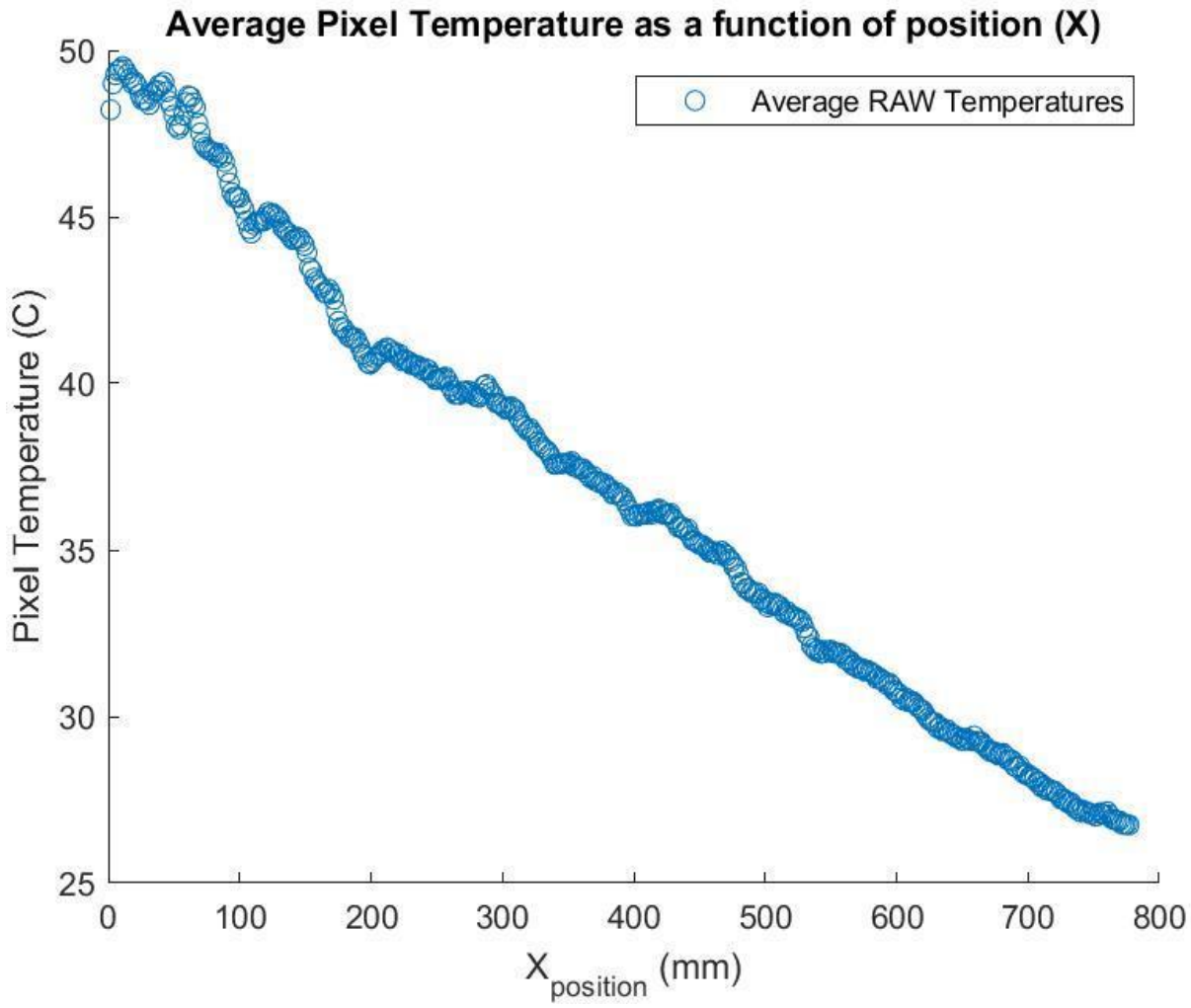

Task 1: Particle Imaging (UNM)

Filtering Thermograms

- Similarly, the filtered thermograms can be fed into PIVlab to perform particle image velocimetry calculations to obtain the particle bulk velocity
  - In our case, the x-component of the velocity is of interest for our calculations

Filtered Thermograms Set

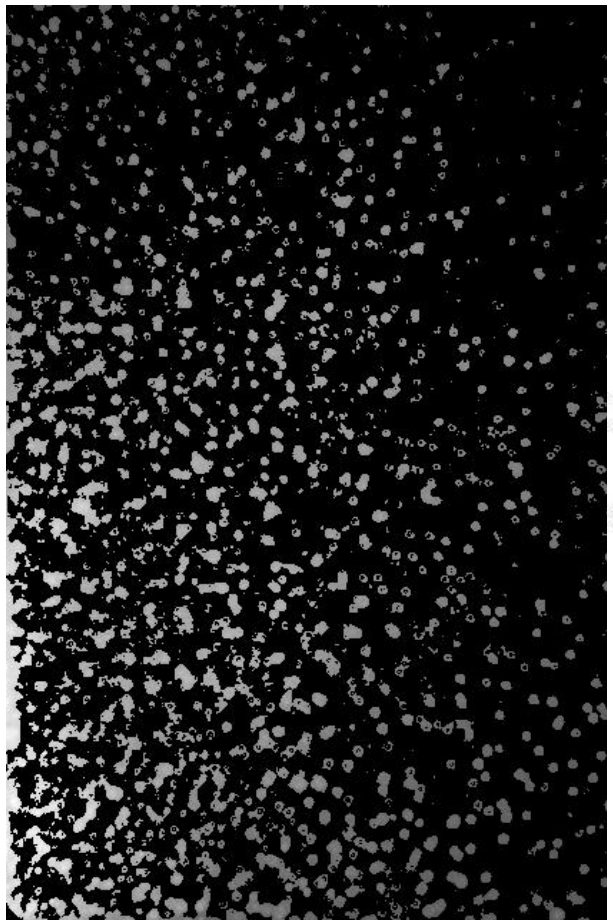

Average X-Velocity

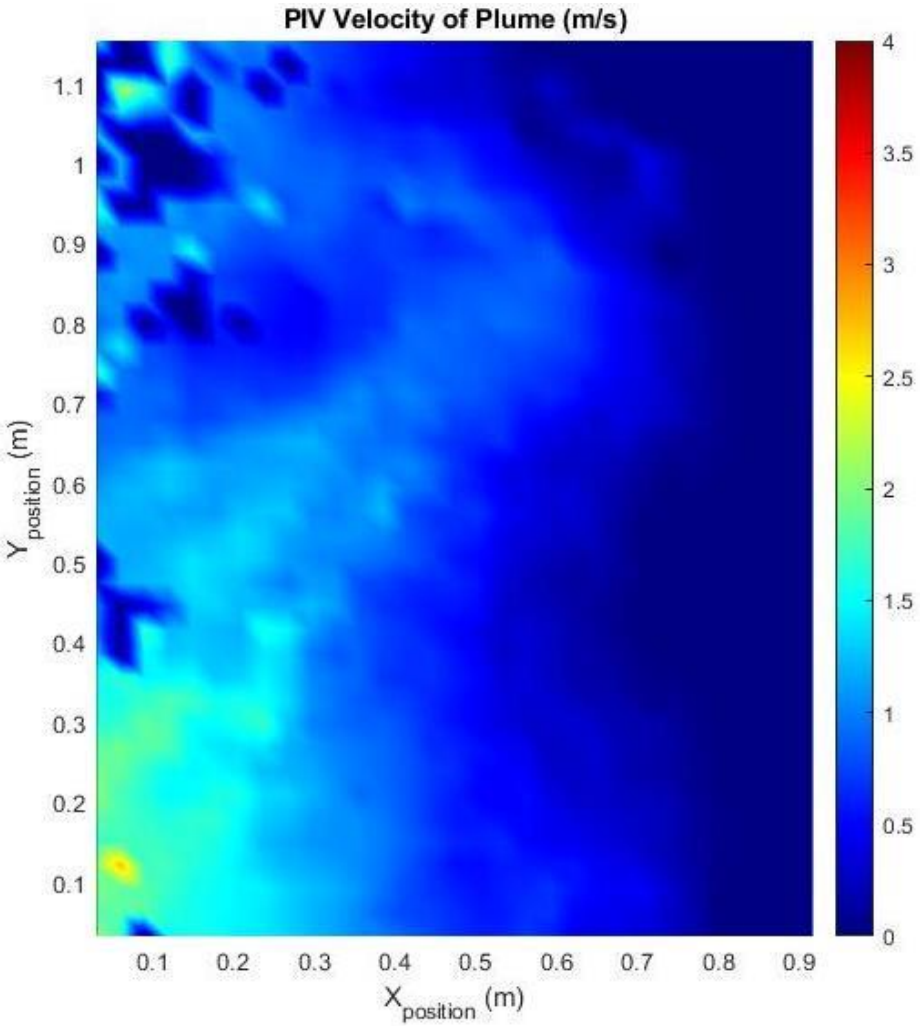

Preliminary On-sun Test Results

Task 1: Particle Imaging (UNM)

Data Analysis

- A 2-minute data set is comprised of 65 visible-light images and 36,000 thermograms (300 fps)
- Every calculation is performed for a single visible-light image and approximately 554 thermograms.
  - Every iteration the average particle temperature and bulk velocity is calculated
  - Lastly, the mass egress rate and heat losses can then be found as seen on the flow schematic

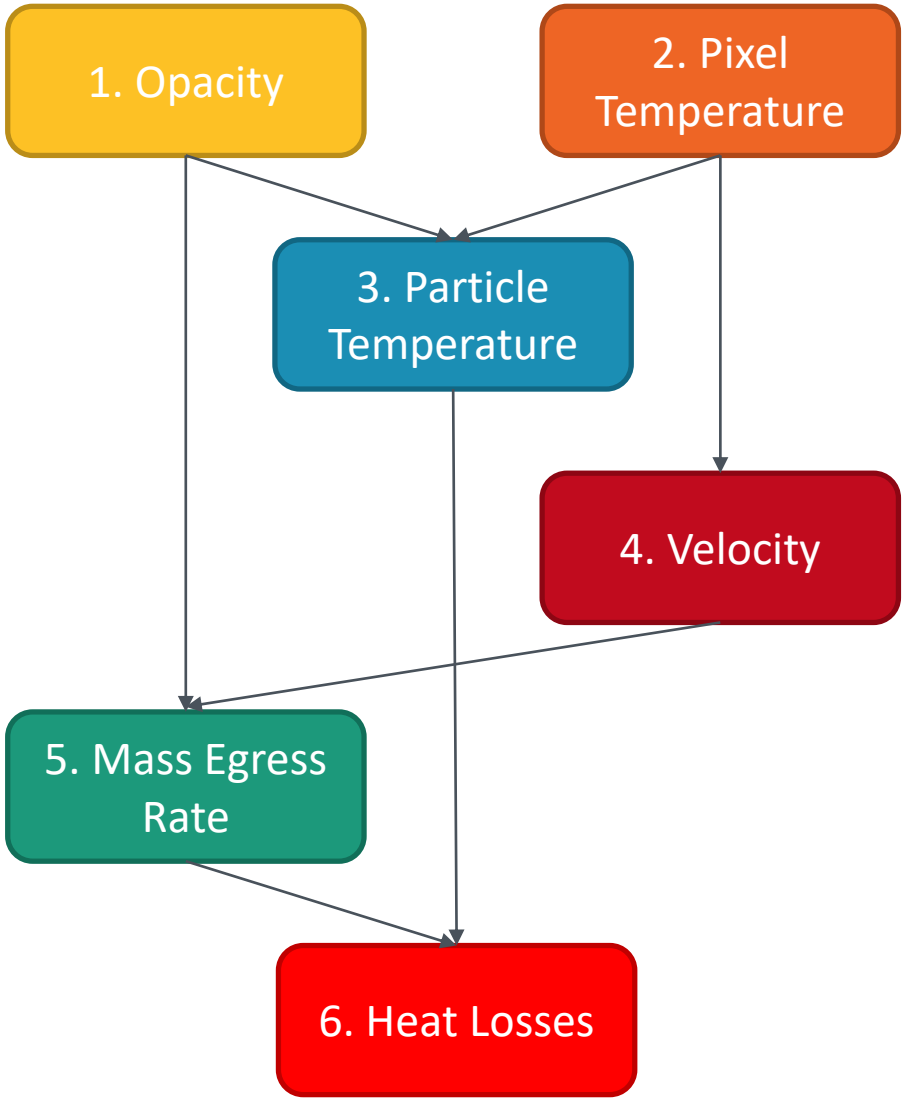

Task 1: Particle Imaging (UNM)

Preliminary On-sun Results

- The team selected a case for which efficiency measurements were performed on September 4th, 2020 at 1:00 pm.
- A 93% expected thermal efficiency with a recorded 494 kW of input power.
- According to Mills and Ho, approximately 70% of the thermal losses from the FPR are due to advective/convective losses.
- This means that from the 35 kW of heat loss, 25 kW would correspond to air and particle advective losses.
  - This value will be used as a reference for our measurements.

Task 1: Particle Imaging (UNM)

Preliminary On-sun Results

- The following represent the opacity and average pixel temperature profiles.
- The calculations will only consider the first 100 mm of flow distance

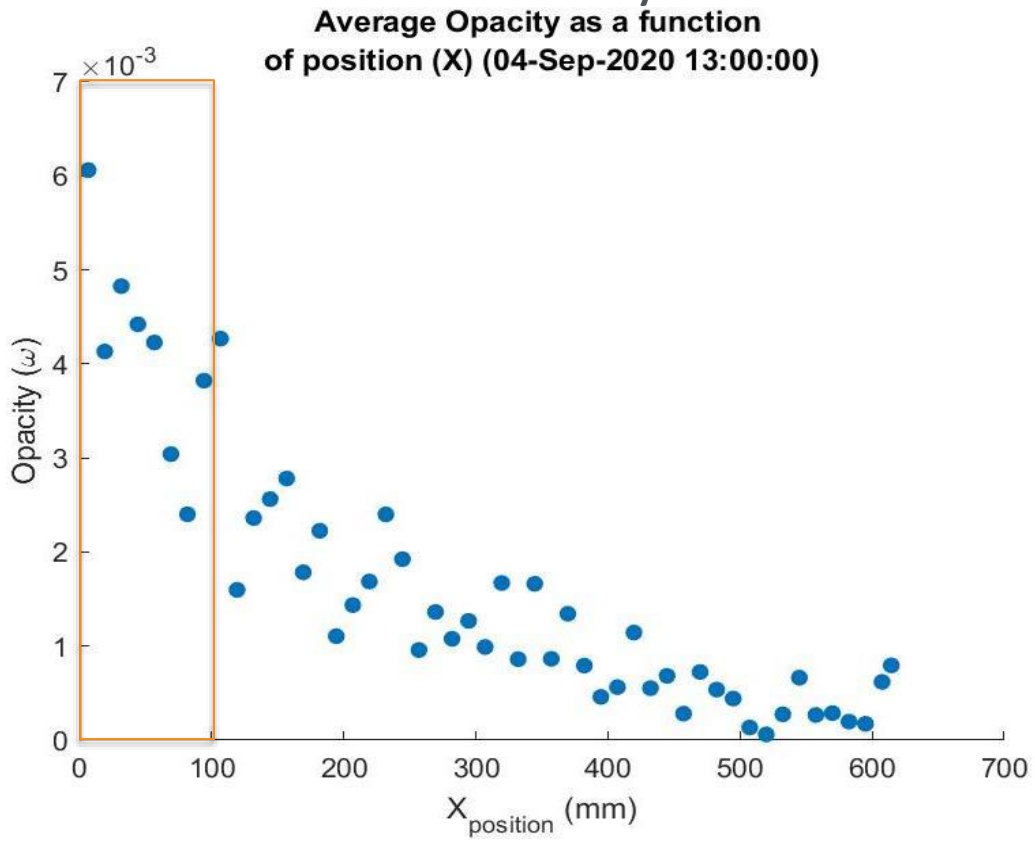

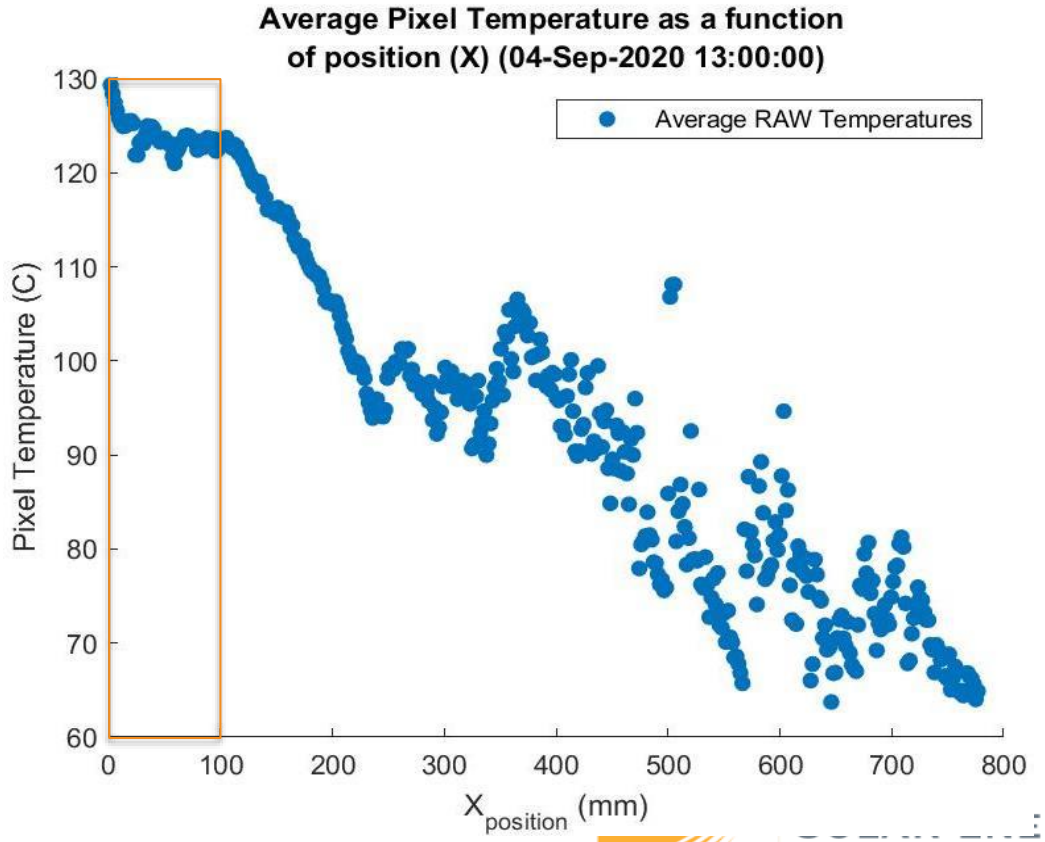

Task 1: Particle Imaging (UNM)

Preliminary On-sun Results

- The following represent the average particle temperature and bulk velocity profiles.
- The calculations will only consider the first 100 mm of flow distance

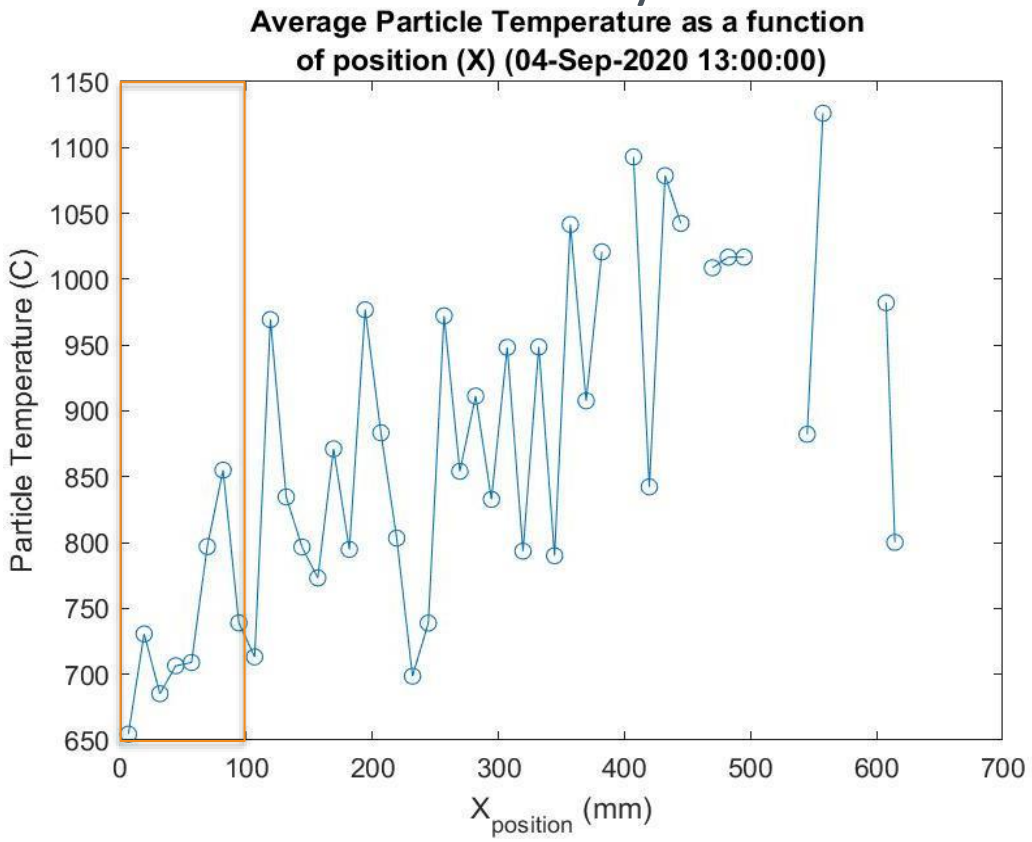

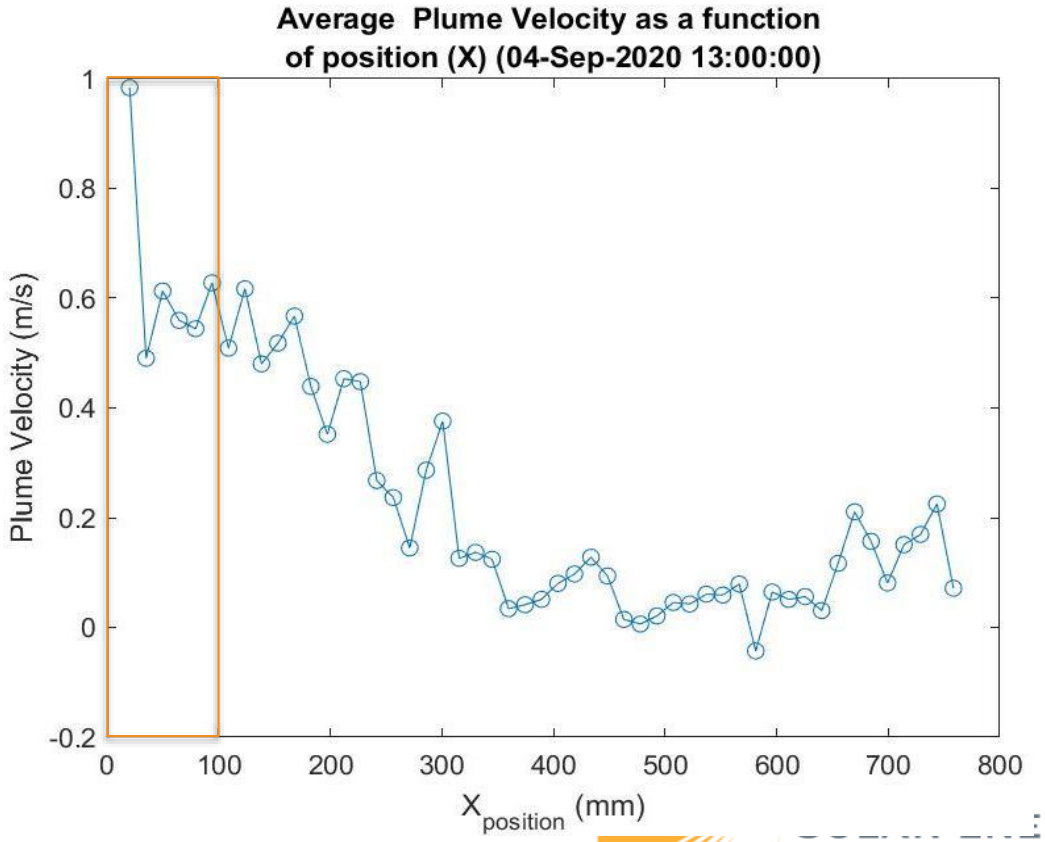

Task 1: Particle Imaging (UNM)

Heat Loss Calculation

- According to Ho and Ortega et al, the heat loss due to the particle and air egress can be found using equation 6 and equation 7, respectively.

$$\dot{Q}_p = \dot{m}_p \int_{T_{amb}}^{T_p} Cp_p(T)dT \quad (6)$$

$$\dot{Q}_a = \dot{m}_a \int_{T_{amb}}^{T_p} Cp_a(T)dT \quad (7)$$

- Where ($\dot{m}$) is the mass flow, the ($Cp(T)$) is the heat capacity as a function of temperature which is integrated from ambient temperature (T_{amb}) to particle temperature (T_p); for air (a) and particles (p).
- The total heat loss can be found applying equation 8.

$$\dot{Q}_T = \dot{Q}_p + \dot{Q}_a \quad (8)$$

Task 1: Particle Imaging (UNM)

Preliminary On-sun Results

- The following represent the average particle emission rate calculated using equation 5 and the heat losses calculated with equation 6

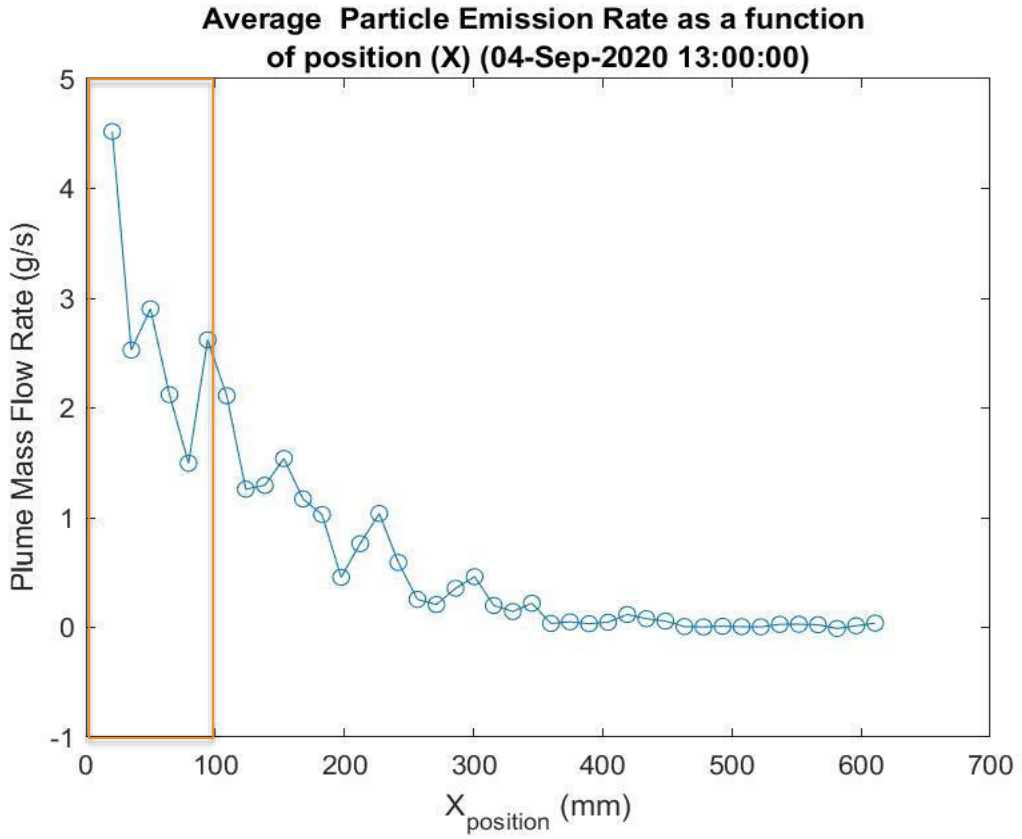

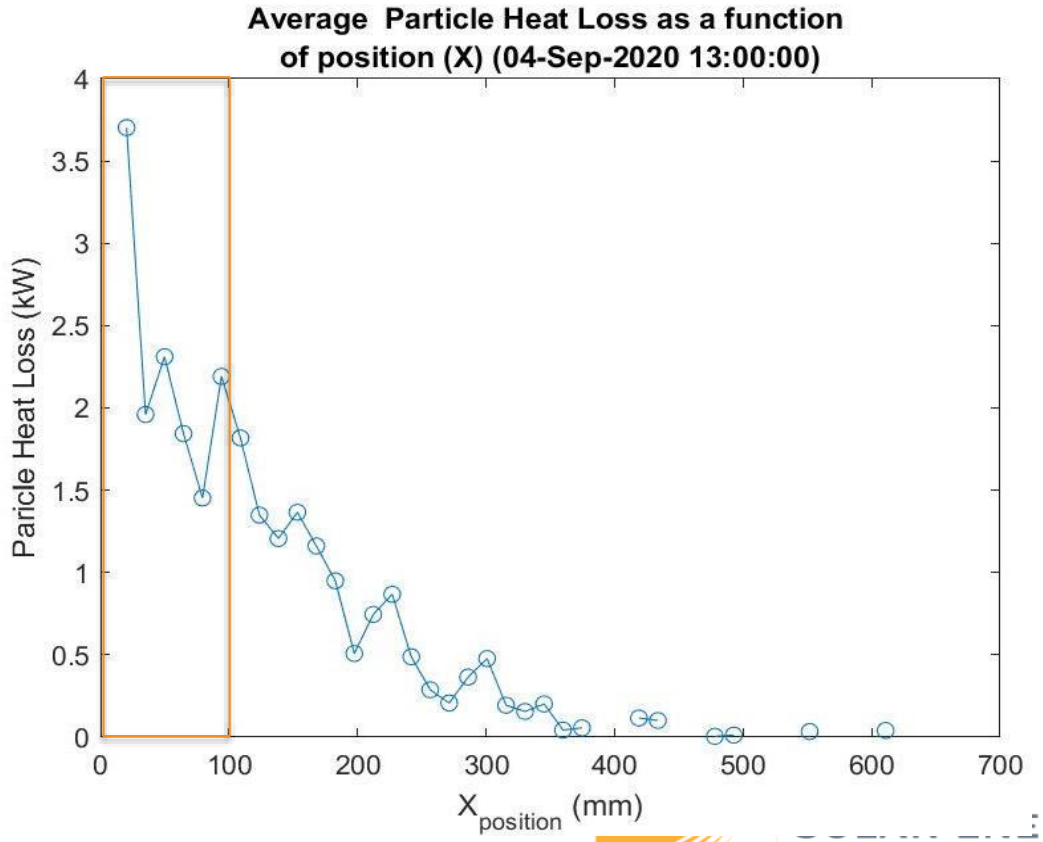

Task 1: Particle Imaging (UNM)

Preliminary On-sun Results

- A chronological chart of the average particle emission rate and particle heat losses for the entire 2 minutes of data show that a approximately 675 g of particle egress and 3.1 kW of thermal losses occurred

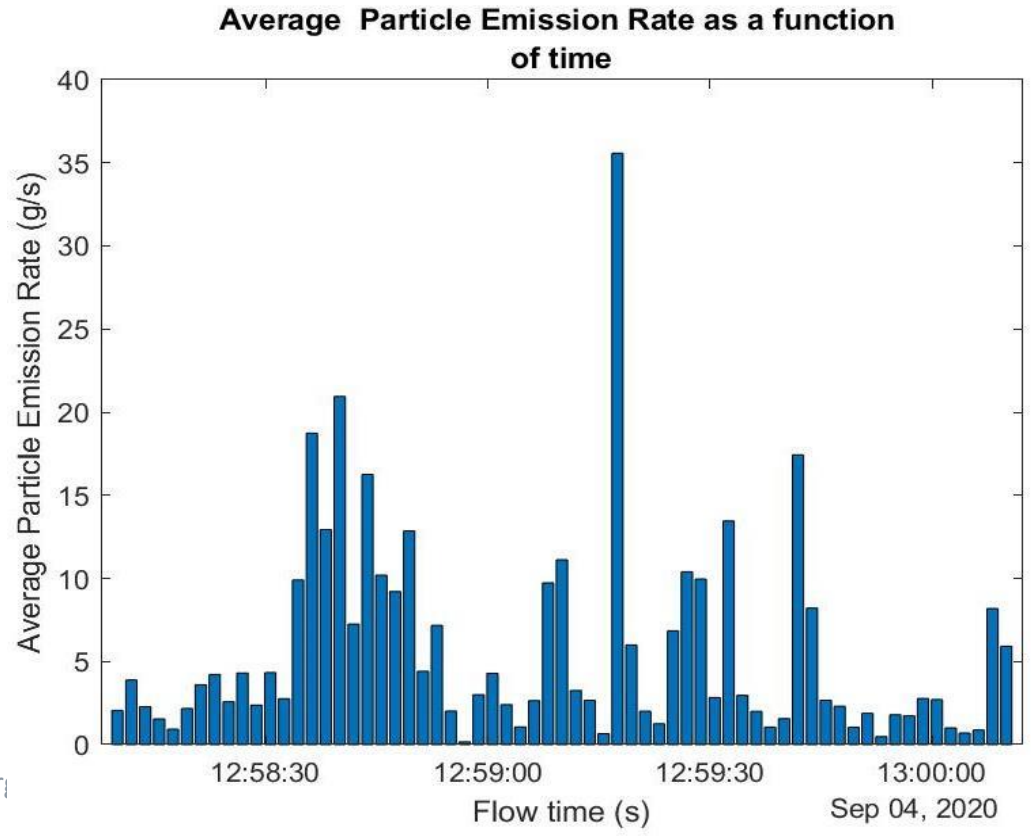

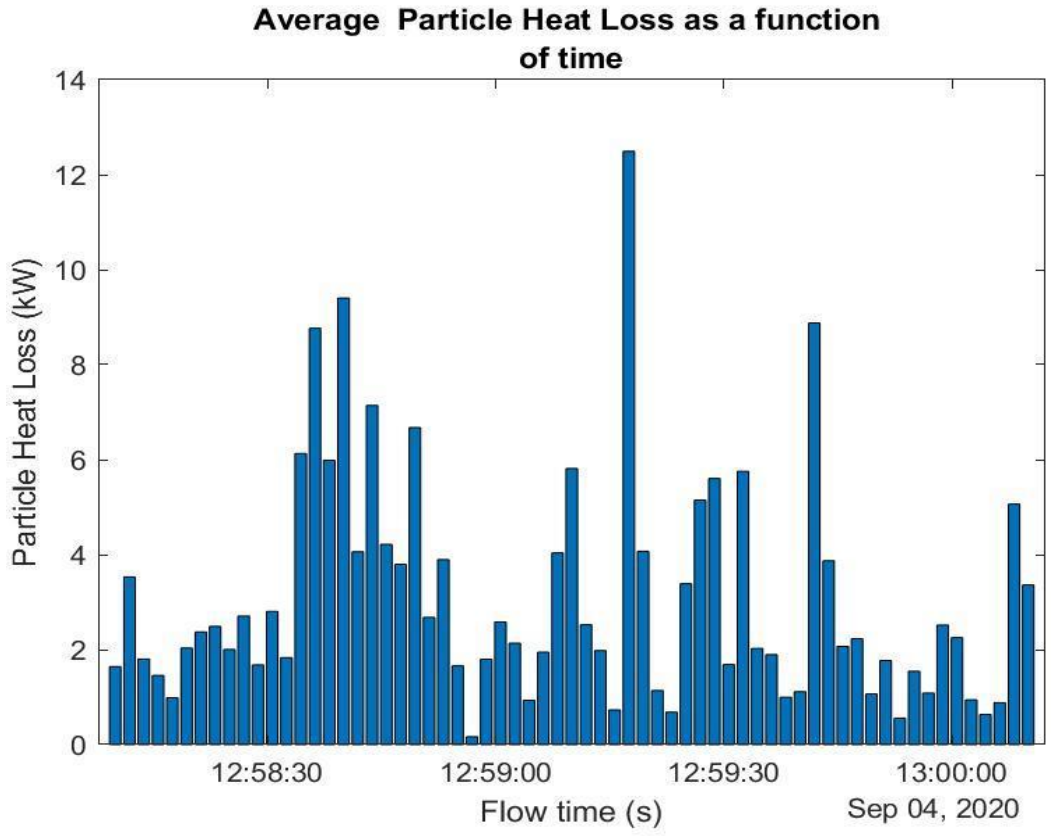

Task 1: Particle Imaging (UNM)

Preliminary On-sun Results

- If the advective losses of air entering/leaving the cavity are considered using the same bulk velocity as a proxy for the air velocity, the chronological plot shows that the total plume heat loss is approximately 61.7 kW.

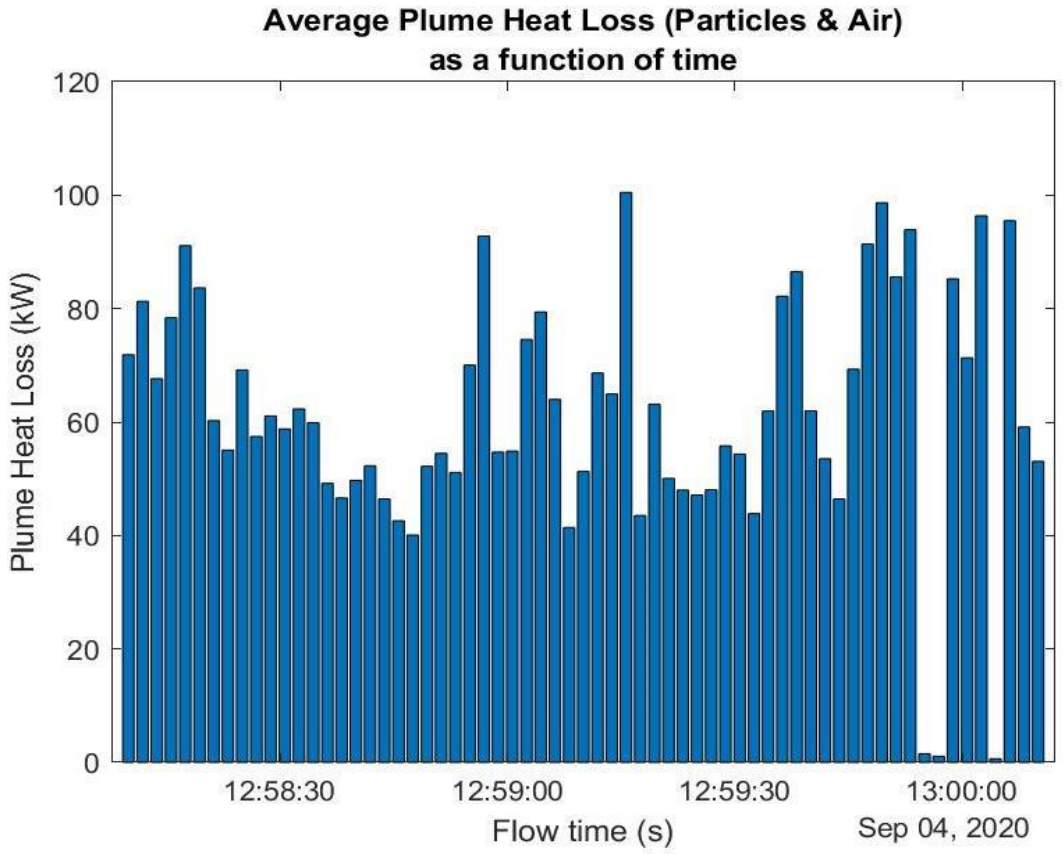

Task 1: Particle Imaging (UNM) – Publications

- Wrote two papers for ASME ES 2021 this past quarter

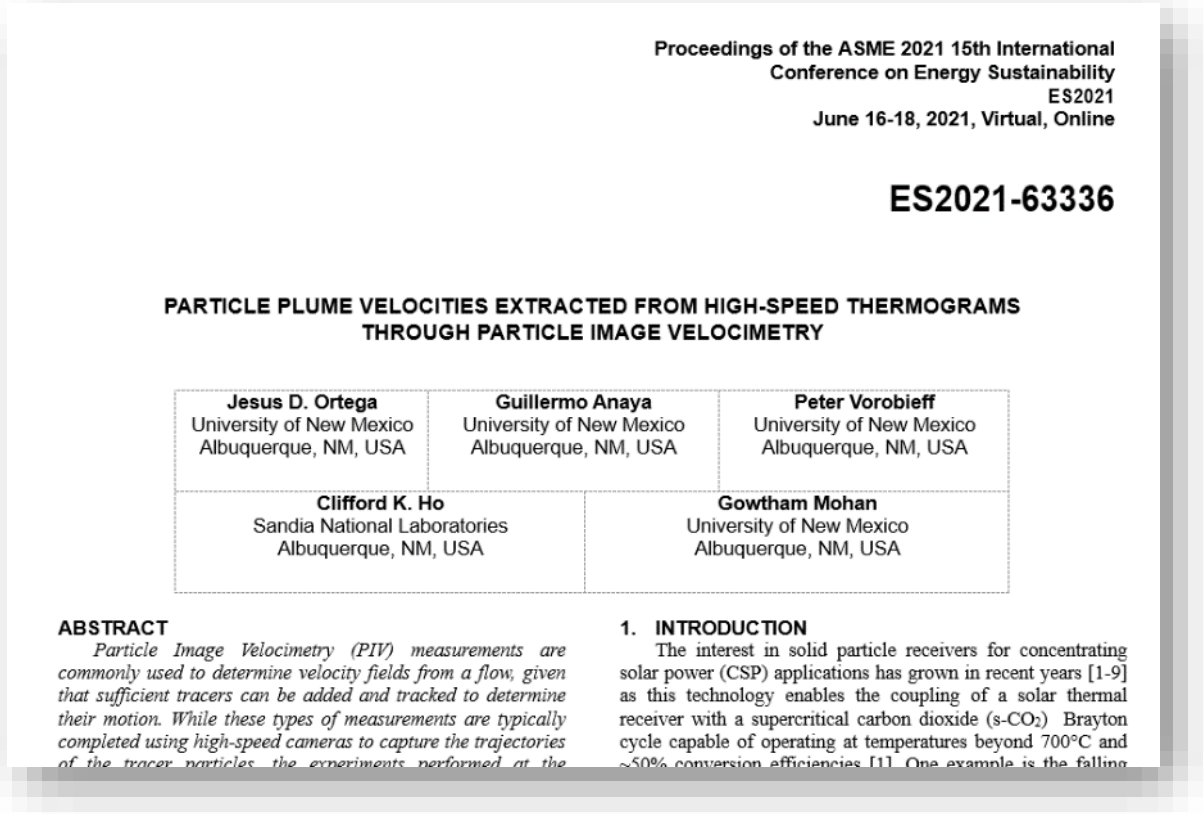

Proceedings of the ASME 2021 15th International
Conference on Energy Sustainability
ES2021
June 16-18, 2021, Virtual, Online

ES2021-63336

PARTICLE PLUME VELOCITIES EXTRACTED FROM HIGH-SPEED THERMOGRAMS THROUGH PARTICLE IMAGE VELOCIMETRY

Jesus D. Ortega
University of New Mexico
Albuquerque, NM, USA

Guillermo Anaya
University of New Mexico
Albuquerque, NM, USA

Peter Vorobieff
University of New Mexico
Albuquerque, NM, USA

Clifford K. Ho
Sandia National Laboratories
Albuquerque, NM, USA

Gowtham Mohan
University of New Mexico
Albuquerque, NM, USA

ABSTRACT

Particle Image Velocimetry (PIV) measurements are commonly used to determine velocity fields from a flow, given that sufficient tracers can be added and tracked to determine their motion. While these types of measurements are typically completed using high-speed cameras to capture the trajectories of the tracer particles, the experiments performed at the

1. INTRODUCTION

The interest in solid particle receivers for concentrating solar power (CSP) applications has grown in recent years [1-9] as this technology enables the coupling of a solar thermal receiver with a supercritical carbon dioxide (s-CO_2) Brayton cycle capable of operating at temperatures beyond 700°C and ~50% conversion efficiencies [1]. One example is the falling

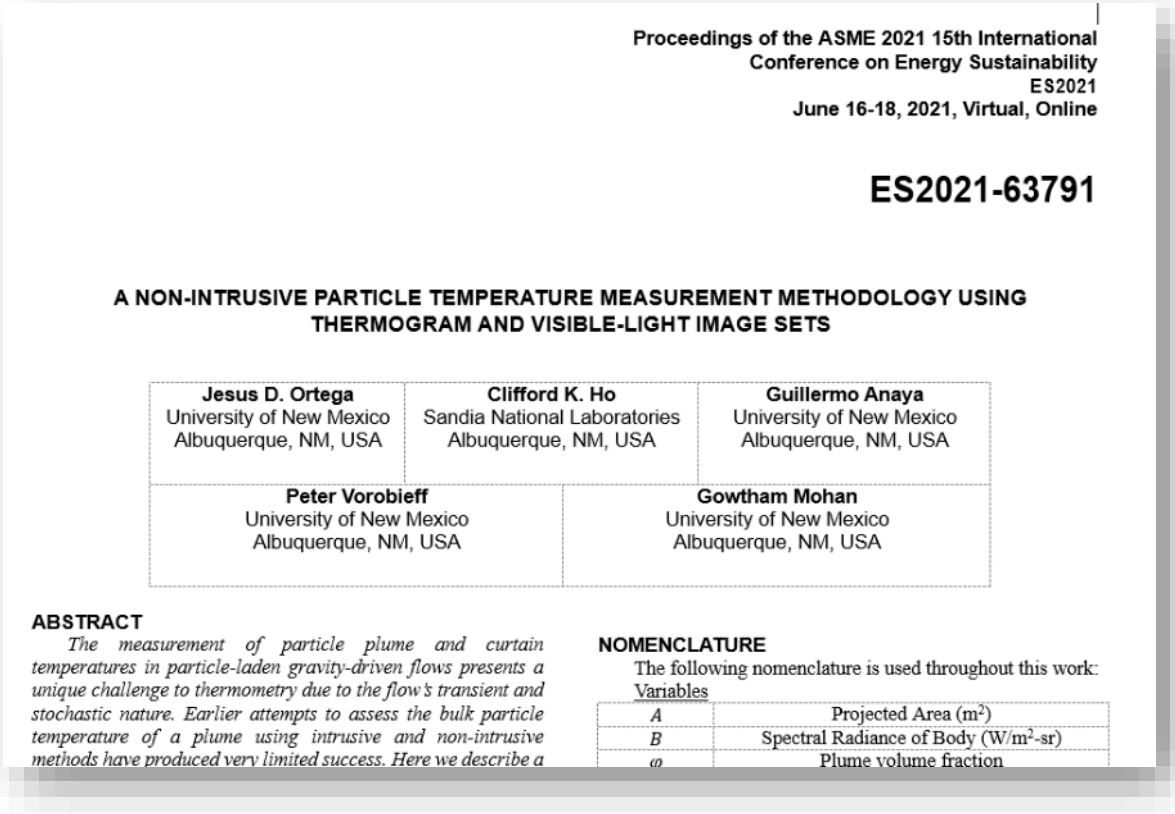

Proceedings of the ASME 2021 15th International
Conference on Energy Sustainability
ES2021
June 16-18, 2021, Virtual, Online

ES2021-63791

A NON-INTRUSIVE PARTICLE TEMPERATURE MEASUREMENT METHODOLOGY USING THERMOGRAM AND VISIBLE-LIGHT IMAGE SETS

Jesus D. Ortega
University of New Mexico
Albuquerque, NM, USA

Clifford K. Ho
Sandia National Laboratories
Albuquerque, NM, USA

Guillermo Anaya
University of New Mexico
Albuquerque, NM, USA

Peter Vorobieff
University of New Mexico
Albuquerque, NM, USA

Gowtham Mohan
University of New Mexico
Albuquerque, NM, USA

ABSTRACT

The measurement of particle plume and curtain temperatures in particle-laden gravity-driven flows presents a unique challenge to thermometry due to the flow's transient and stochastic nature. Earlier attempts to assess the bulk particle temperature of a plume using intrusive and non-intrusive methods have produced very limited success. Here we describe a

NOMENCLATURE

The following nomenclature is used throughout this work:

Variables

A	Projected Area (m^2)
B	Spectral Radiance of Body (W/m^2-sr)
φ	Plume volume fraction

Task 1: Particle Imaging (UNM) – Summary and Next Steps

- A post-processing code has been completed to apply the methodology developed to estimate the mass and heat losses from the FPR during operation.
- As shown, the estimates obtained using the methodology align well with the predicted values during the on-sun tests.
- We will continue to look at these discrete cases to compare the efficiencies predilected and those stimmed using the imaging methodology.
- Similarly, we will continue to post-process the on-sun test data collected to build a clearer picture of the sampling frequency required and to try and develop a correlation between the particle egress and the cavity/wind conditions during on-sun tests.

Task 2 – Particle Sampling

Near-Field and Far-Field Sampling

- Quantify particle emissions using standard (and new) air monitoring procedures and compare to OSHA and EPA standards
- Perform both near-field (tower top) and far-field (tethered balloons) sampling

Near-Field Particle Sampling

- Presented in last quarterly report (BP2 Q6)
- Published results in ASME ES2021 paper this past quarter

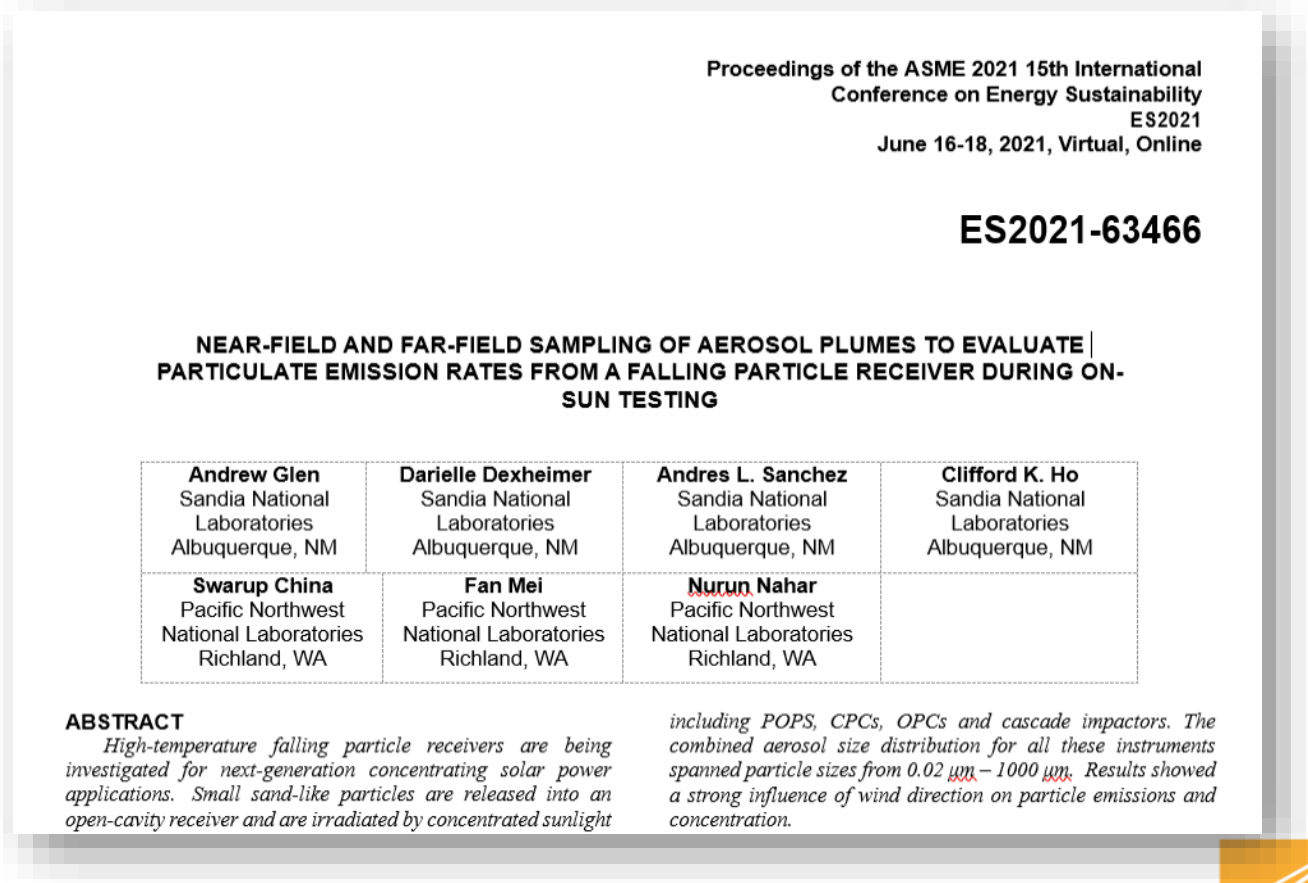

Proceedings of the ASME 2021 15th International
Conference on Energy Sustainability
ES2021
June 16-18, 2021, Virtual, Online

ES2021-63466

NEAR-FIELD AND FAR-FIELD SAMPLING OF AEROSOL PLUMES TO EVALUATE PARTICULATE EMISSION RATES FROM A FALLING PARTICLE RECEIVER DURING ON-SUN TESTING

Andrew Glen Sandia National Laboratories Albuquerque, NM	**Darielle Dexheimer** Sandia National Laboratories Albuquerque, NM	**Andres L. Sanchez** Sandia National Laboratories Albuquerque, NM	**Clifford K. Ho** Sandia National Laboratories Albuquerque, NM
Swarup China Pacific Northwest National Laboratories Richland, WA	**Fan Mei** Pacific Northwest National Laboratories Richland, WA	**Nurun Nahar** Pacific Northwest National Laboratories Richland, WA	

ABSTRACT

High-temperature falling particle receivers are being investigated for next-generation concentrating solar power applications. Small sand-like particles are released into an open-cavity receiver and are irradiated by concentrated sunlight including POPS, CPCs, OPCs and cascade impactors. The combined aerosol size distribution for all these instruments spanned particle sizes from 0.02 μm – 1000 μm. Results showed a strong influence of wind direction on particle emissions and concentration.

Particle Sampling Instrumentation Locations

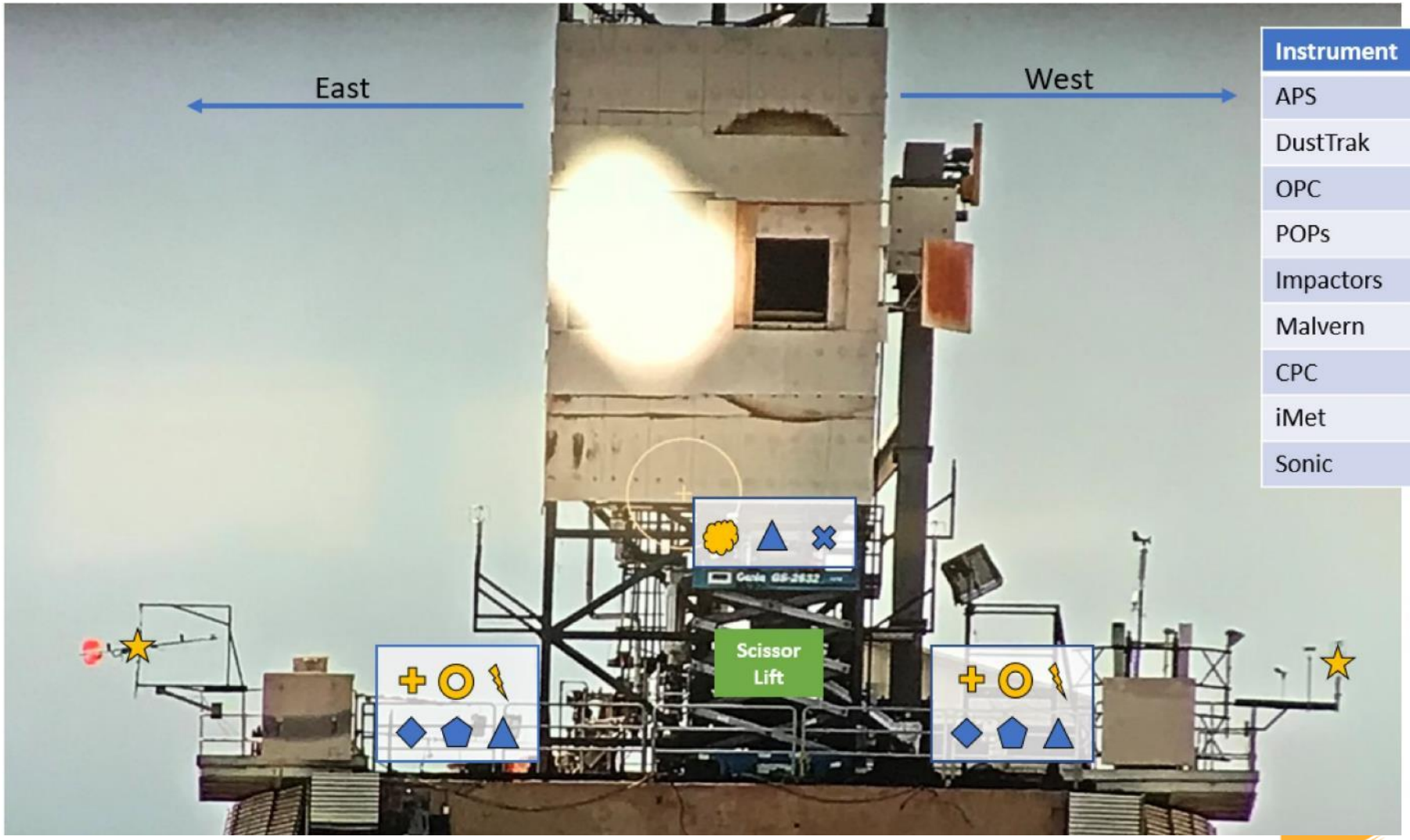

Instrument	Min Size	Max Size
APS	0.5 µm	20 µm
DustTrak	1 µm	15 µm
OPC	0.3 µm	7 µm
POPs	0.14 µm	3 µm
Impactors	0.25, 0.5, 1.0, 2.5 µm	
Malvern	0.5 µm	1000 µm
CPC	20 nm	
iMet	N/A – Met variables	
Sonic	N/A – Met variables	

Particle Sampling Equipment

Equipment	Description	Pros	Cons
Malvern SprayTec	Real-time measurements with a particle size range of 0.1-2000µm. In this case, the sensor would be placed a close to the source as possible by utilizing a scissor lift.	Real-time particle size measurements	Only one system available, instrument protection is a factor, and placement of the system will depending on wind speed/direction. Dependent on Mie Scattering.
TSI Aerodynamic Particle Sizer (APS)	Real-time measurement with size range from 0.5-20µm. Measurement based on time-of-flight of airborne particulates.	Real-time particle size measurements. Multiple units available.	Point source sensor. No speciation.
Alphasense Optical Particle Counter (OPC)	Optical particle monitor that measure PM 1.0, 2.5, and 10.	Light weight, inexpensive, and used for outdoor air quality measurements with low power consumption. Multiple units available.	Not as sensitive/accurate as other optical equipment. No speciation.
TSI DustTrak Aerosol Monitor	Real-time dust monitoring which measures size-segregated mass fraction concentrations corresponding to PM1, 2.5, 10, and total size fractions.	Real-time measurement that is environmentally protected and can run on batteries. Aerosol conc. Range 0.001 to 150 mg/m^3. Multiple units available.	Size fraction limited and no speciation.
4- Stage Cascade Impactor	These units can provide particle size information from 0.5-2.5µm. This system is based on the weight of material deposited at each stage.	Particle size fractionation and can be used to determine speciation (chemical/SEM imaging)	Not real-time measurements
Handix Scientific Portable Optical Particle Spectrometer (POPS)	These units can provide particle size information from 0.13-3.0µm using single particle light-scattering. Often used for unmanned aerial platforms and clean rooms.	Light-weight, high-sensitivity, rugged design and low power consumption.	Size limited and point source sensor.
TSI Condensation Particle Counter (CPC)	This unit can provide concentration measurements of particles sizes between 0.01 to >1.0µm.	Light-weight and often used for inhalation/exposure studies.	System uses isopropyl alcohol as working fluid, so it can dry out in harsh conditions. It is also size limited.

Particle Tipping Bucket

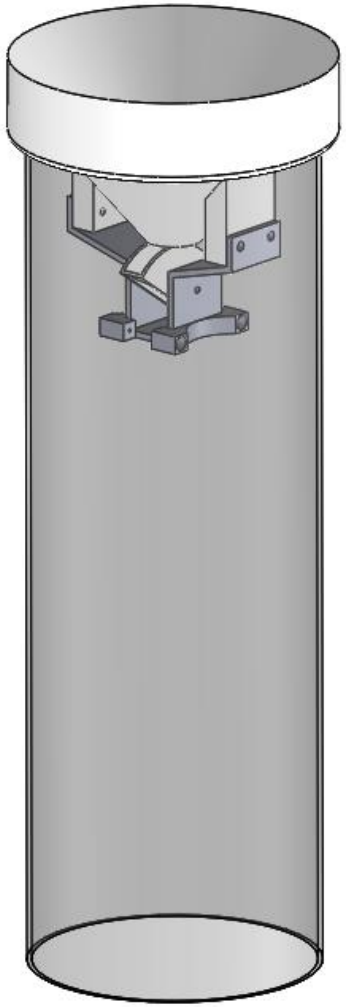

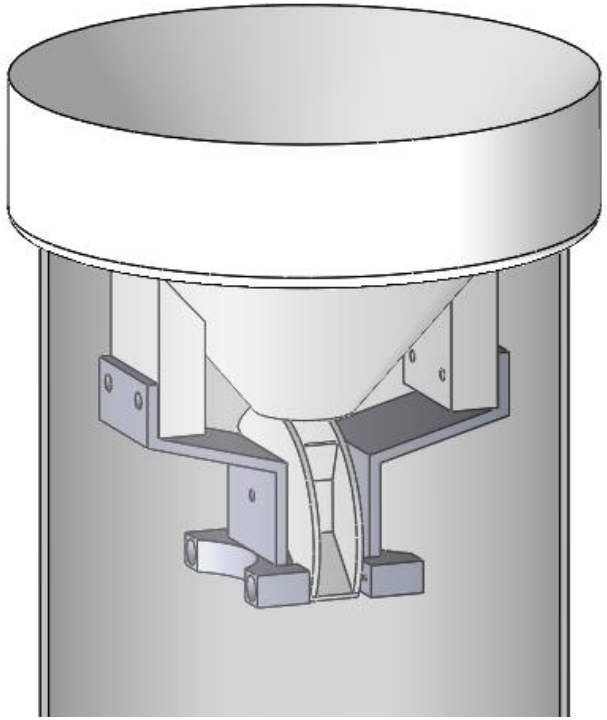

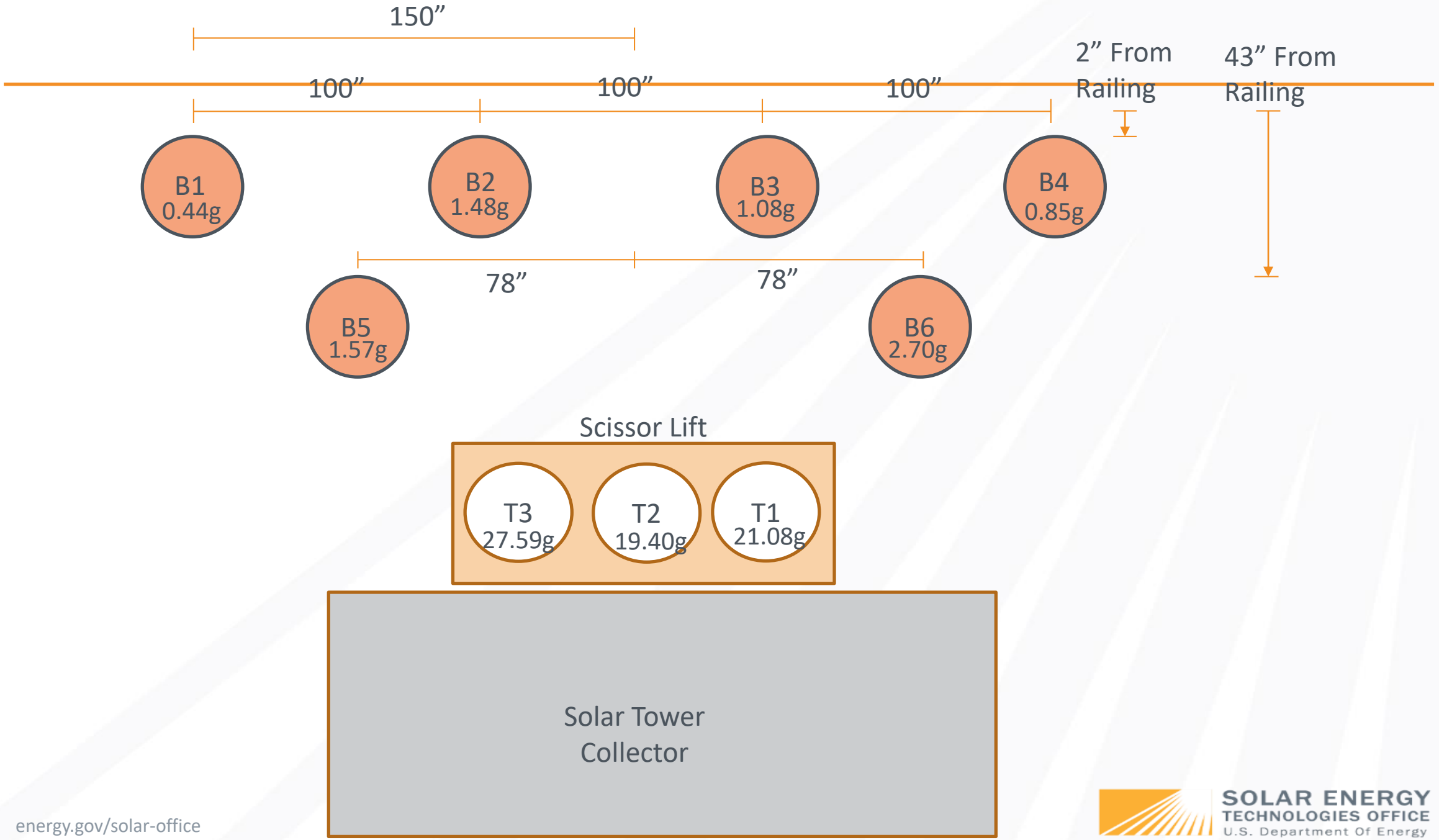
150”
100”
100”
100”
2” From Railing
43” From Railing
B1
0.44g
B2
1.48g
B3
1.08g
B4
0.85g
78”
78”
B5
1.57g
B6
2.70g
Scissor Lift
T3
27.59g
T2
19.40g
T1
21.08g
Solar Tower Collector

Particle Morphology

- Particle Morphology using SEM

Pristine CarboHSP[1]

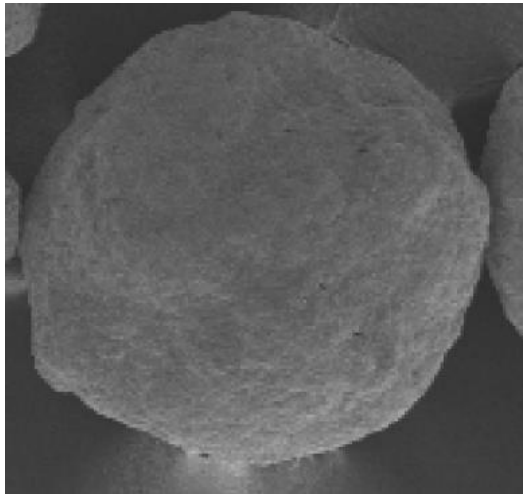

Impactor Sample 1

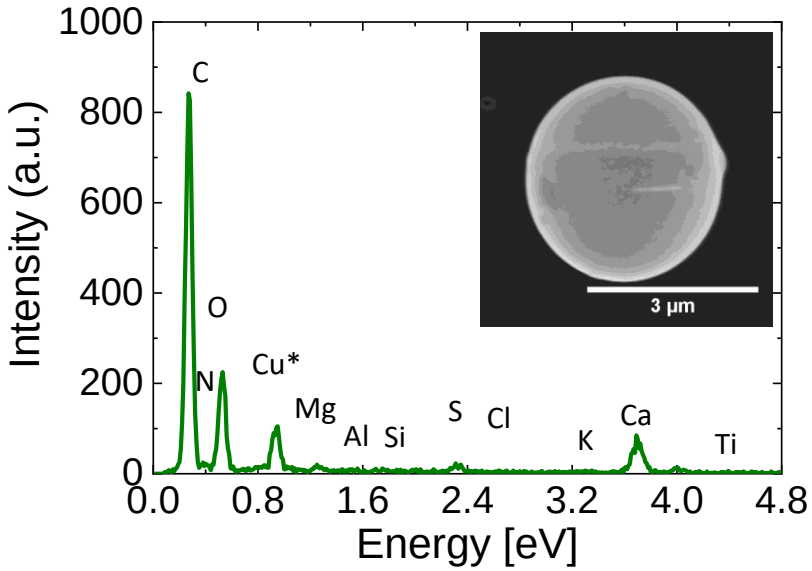

Impactor Sample 2

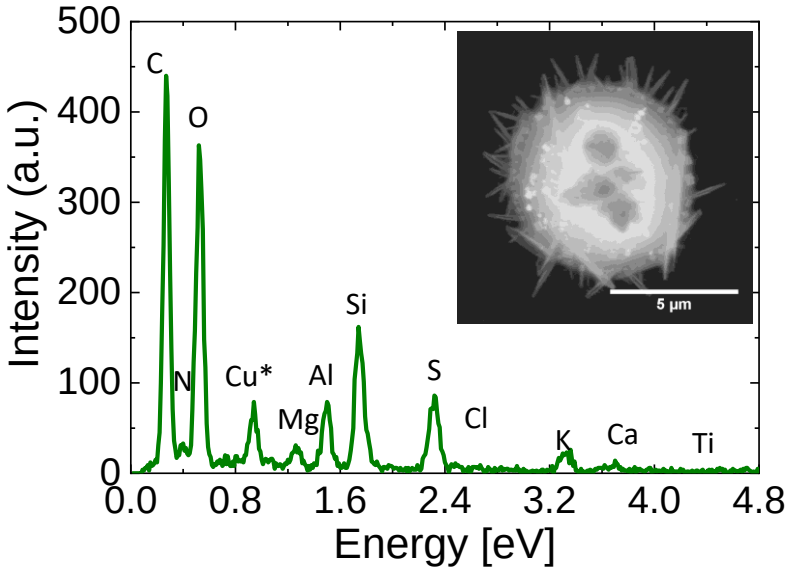

Distinct differences between particle morphology.
Protrusions from agglomerated material generated from the process or crustal material from the atmosphere.

[1] Martins, Vanderlei.,AirPhoton - Electron Microscopy Analysis of the CARBO particles, Personal Communication, (2020)

Far-Field Sampling – Tethered Balloon System

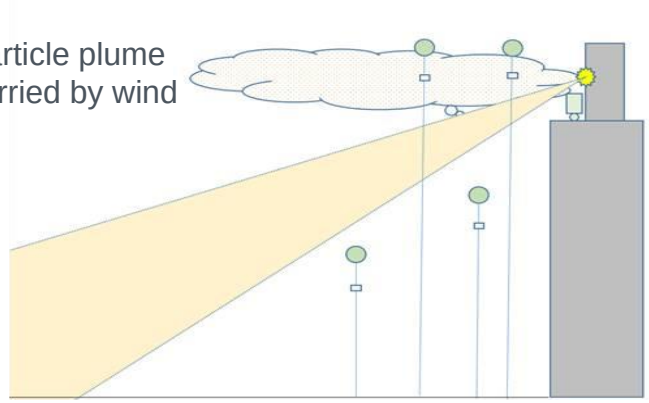

- Far-field sampling deployed multiple instrumented tethered balloons
- Results will help quantify the horizontal and spatial homogeneity of particle emission with respect to wind speed, wind direction, and distance from the aperture

Far-Field Sampling – Tethered Balloon System

- Far-field sampling took place on November 3, 2020
- Three tethered balloons combined with near-field sampling
- Two static and one profiler (Downwind 1)

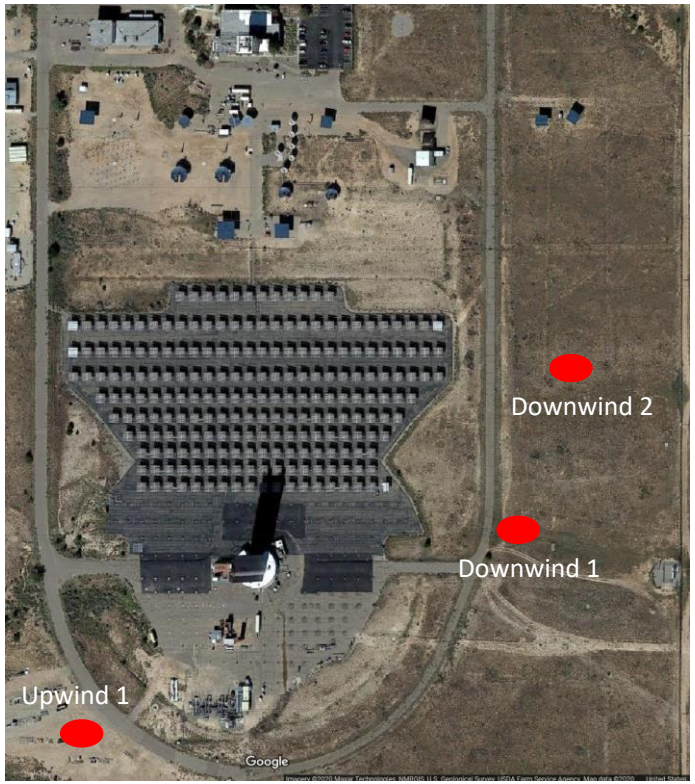

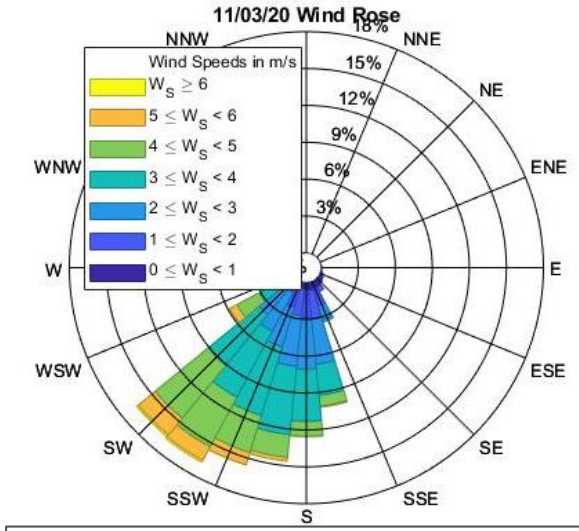

Balloon instrumentation captured impacts from the tower.
Combination of instruments per balloon.

Meteorological Conditions

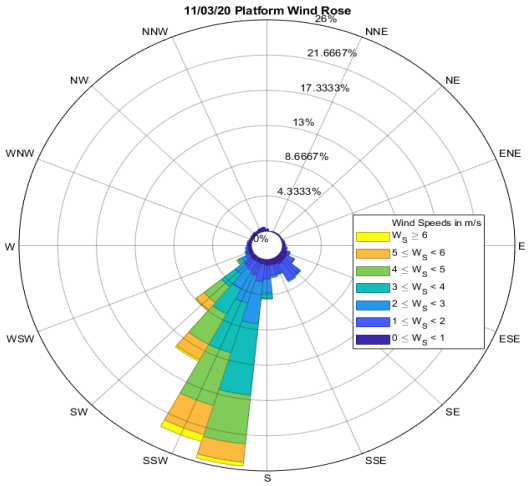

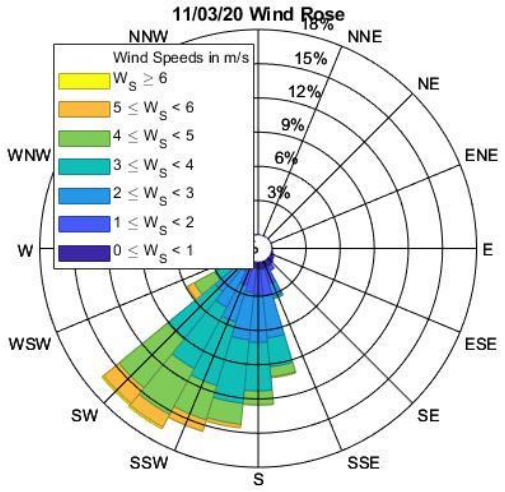

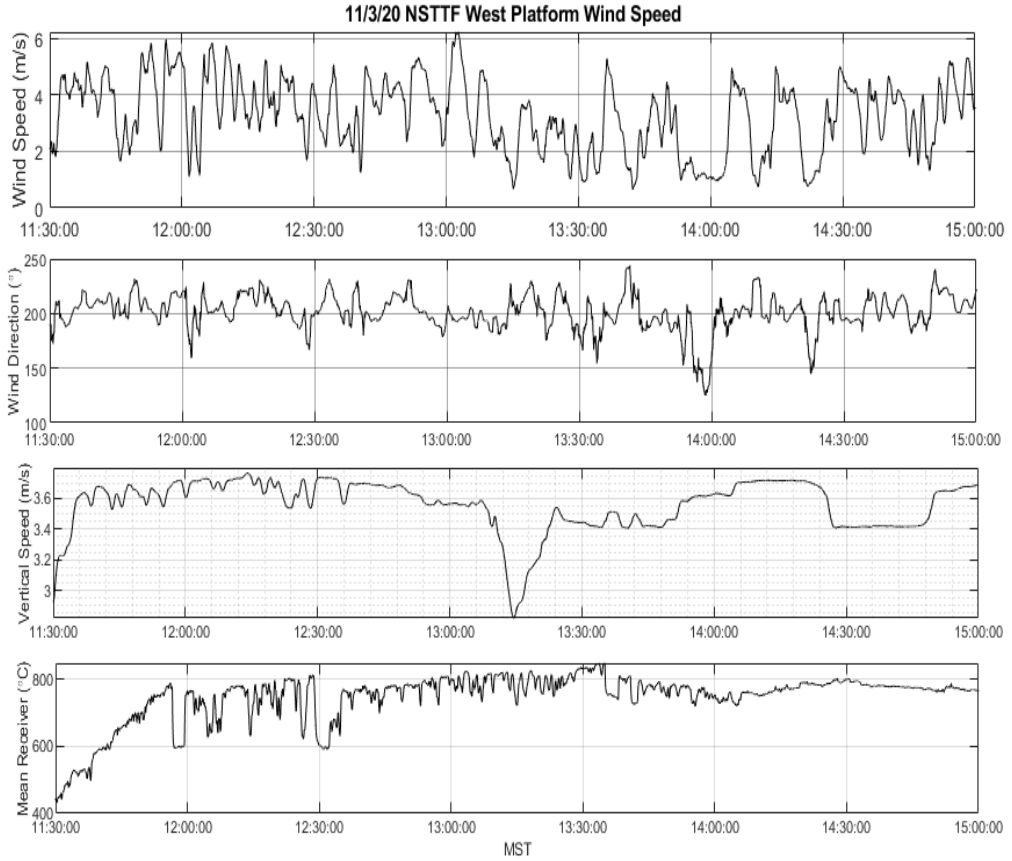

Far-field testing is highly dependent on ambient meteorological conditions.
Forecast for November 3, 2020 indicated good conditions.

Far-Field Flight Tracks

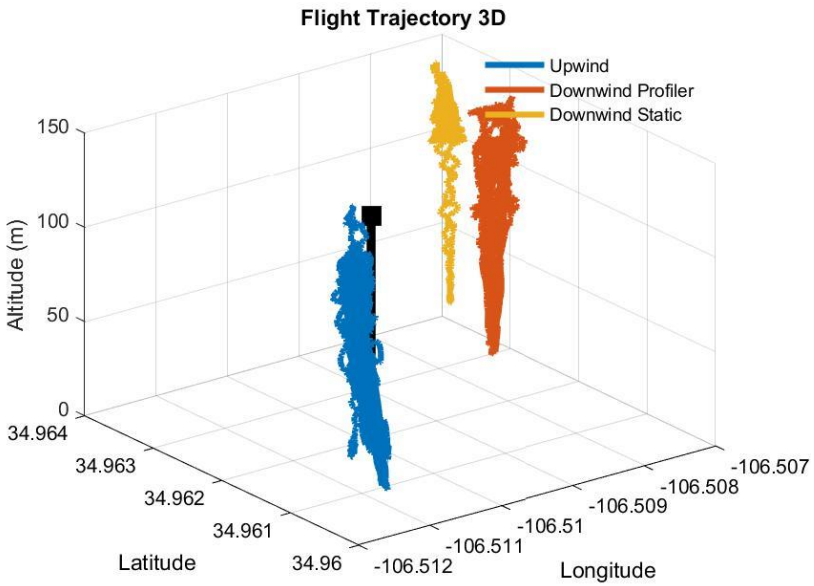

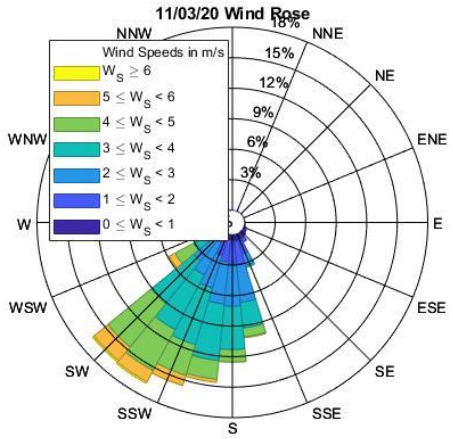

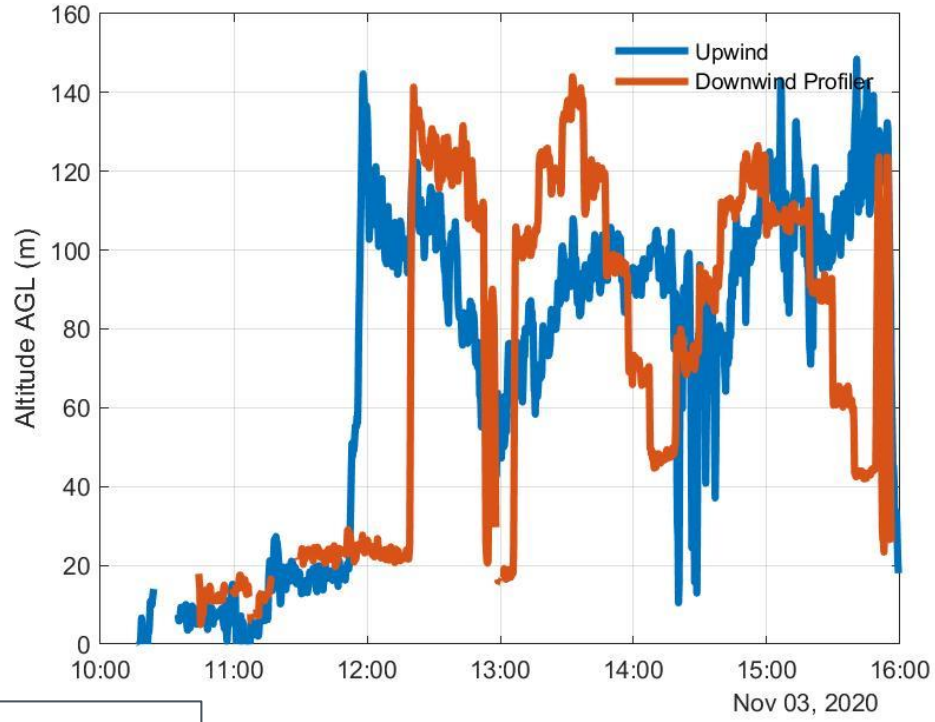

Three balloons to target different wind vectors, increase chance of capturing plume.
Downwind profiler was used to target multi-levels.

Upwind to Near-Field Comparison: POPS

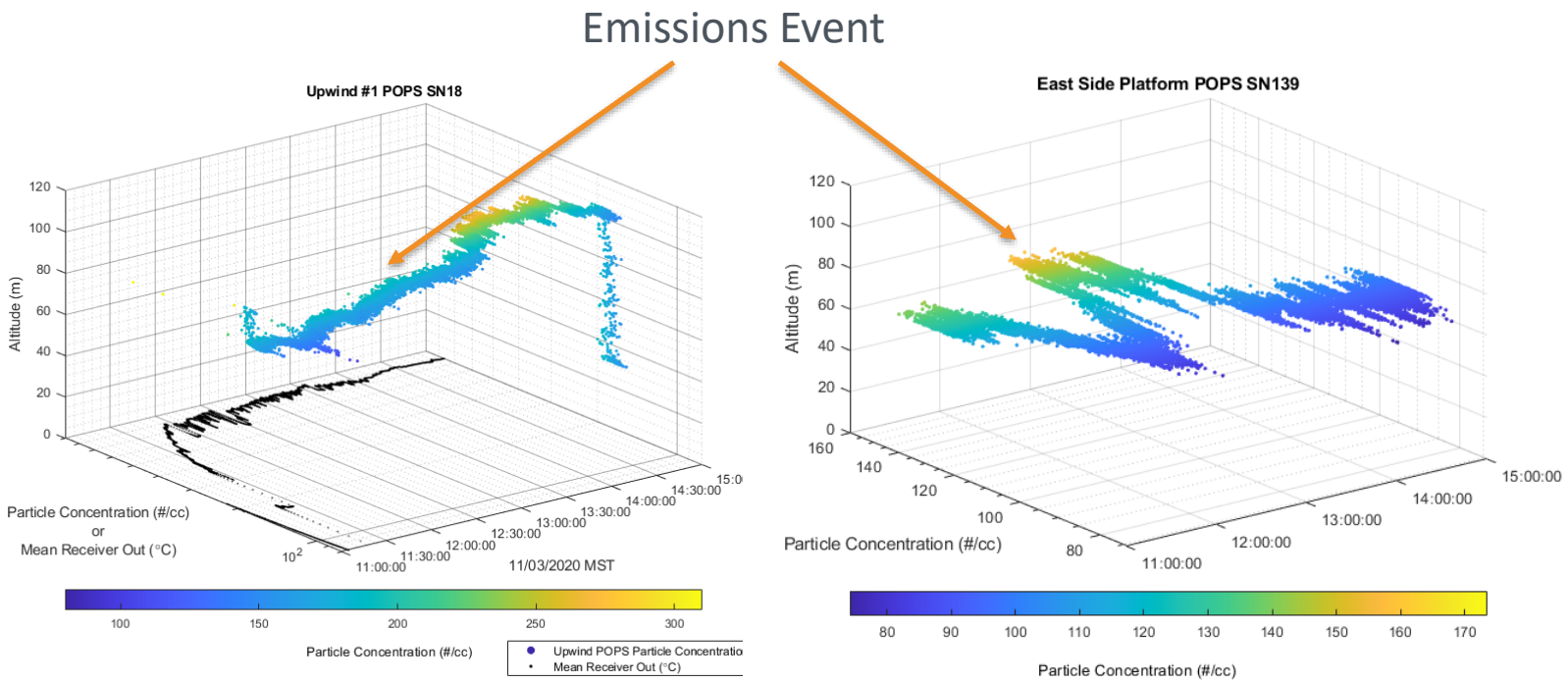

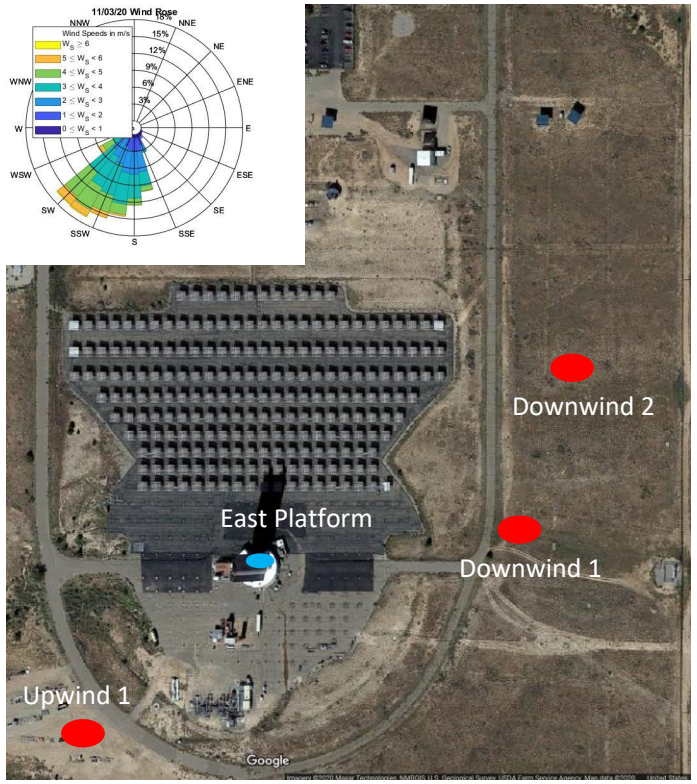

Discrete events where the tower east POPS saw increased concentrations of larger particles (0.14 µm > Dp > 3 µm).

Far-Field Sampling: Upwind to Downwind 2 - CPC

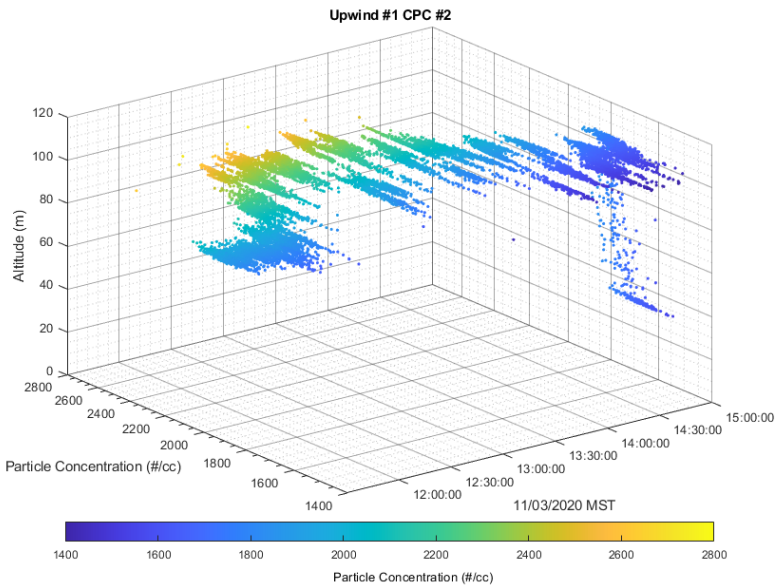

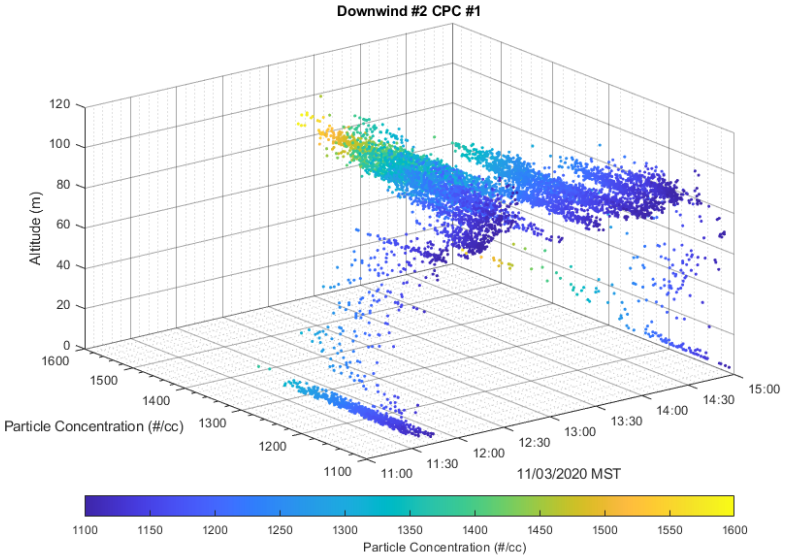

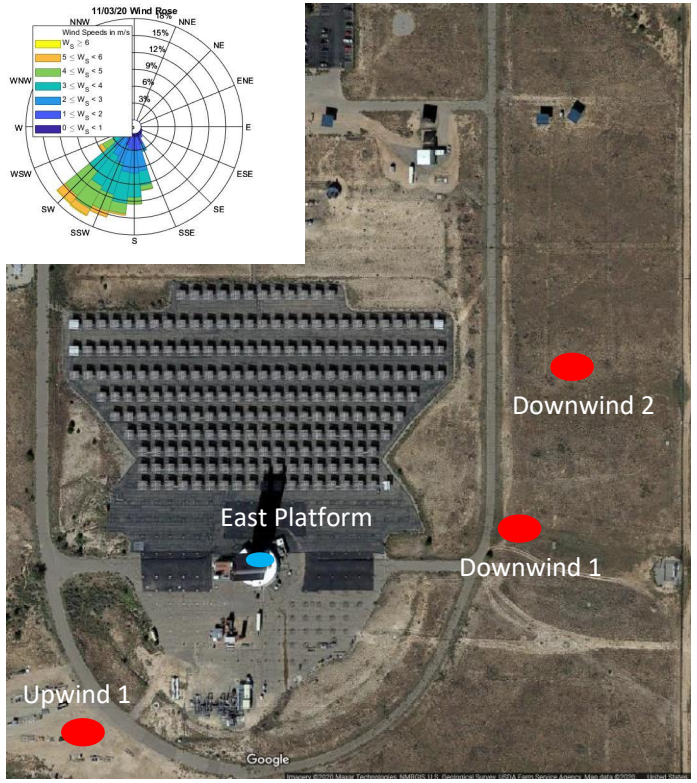

Upwind concentrations of small particles (0.01 µm > Dp > 1 µm) significantly higher than Downwind 2. (Note not the same axis).

Far-Field Sampling: Upwind – Near-Field – Downwind 1

- Alphasense OPCs
- Profiling Balloon

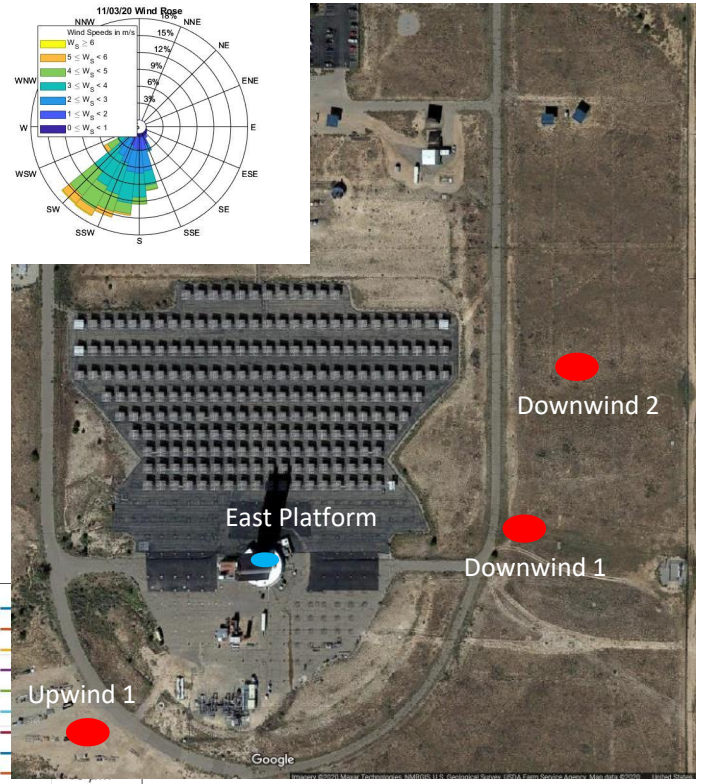

Upwind OPC

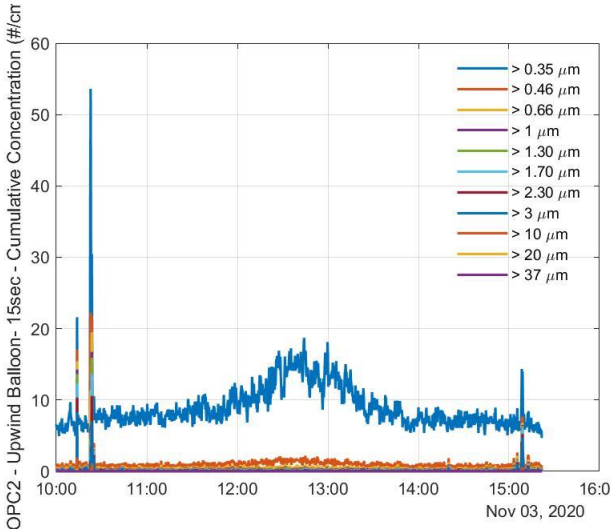

Tower East OPC

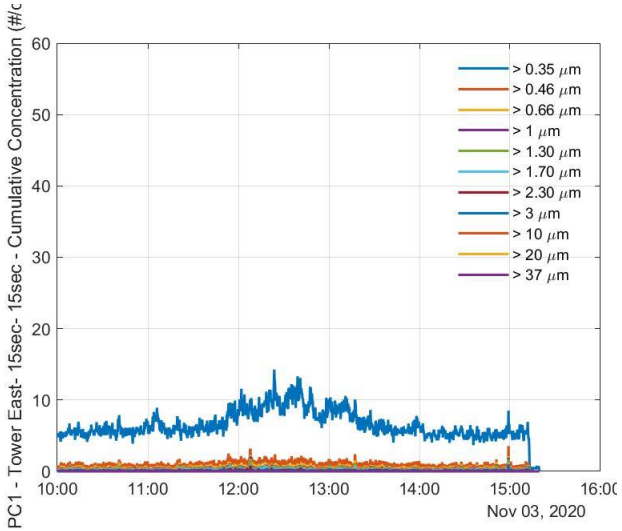

Downwind 1 OPC

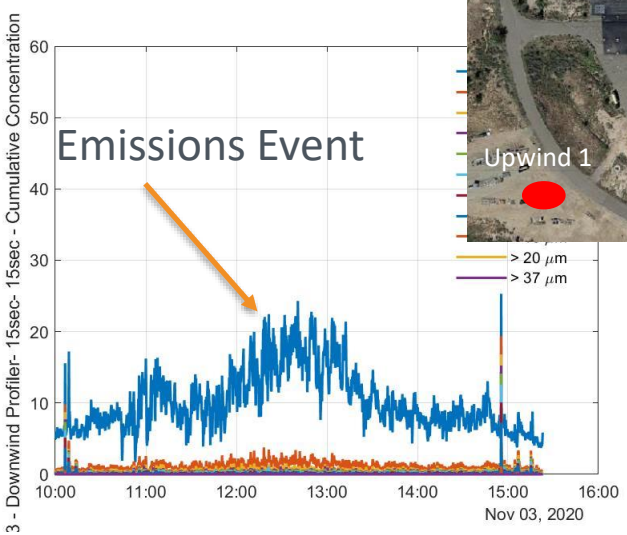

Slight increase in concentrations measured by Downwind 1 OPC (0.35 µm > Dp > 37 µm).

Far-Field Sampling: Upwind – Near-Field – Downwind 2

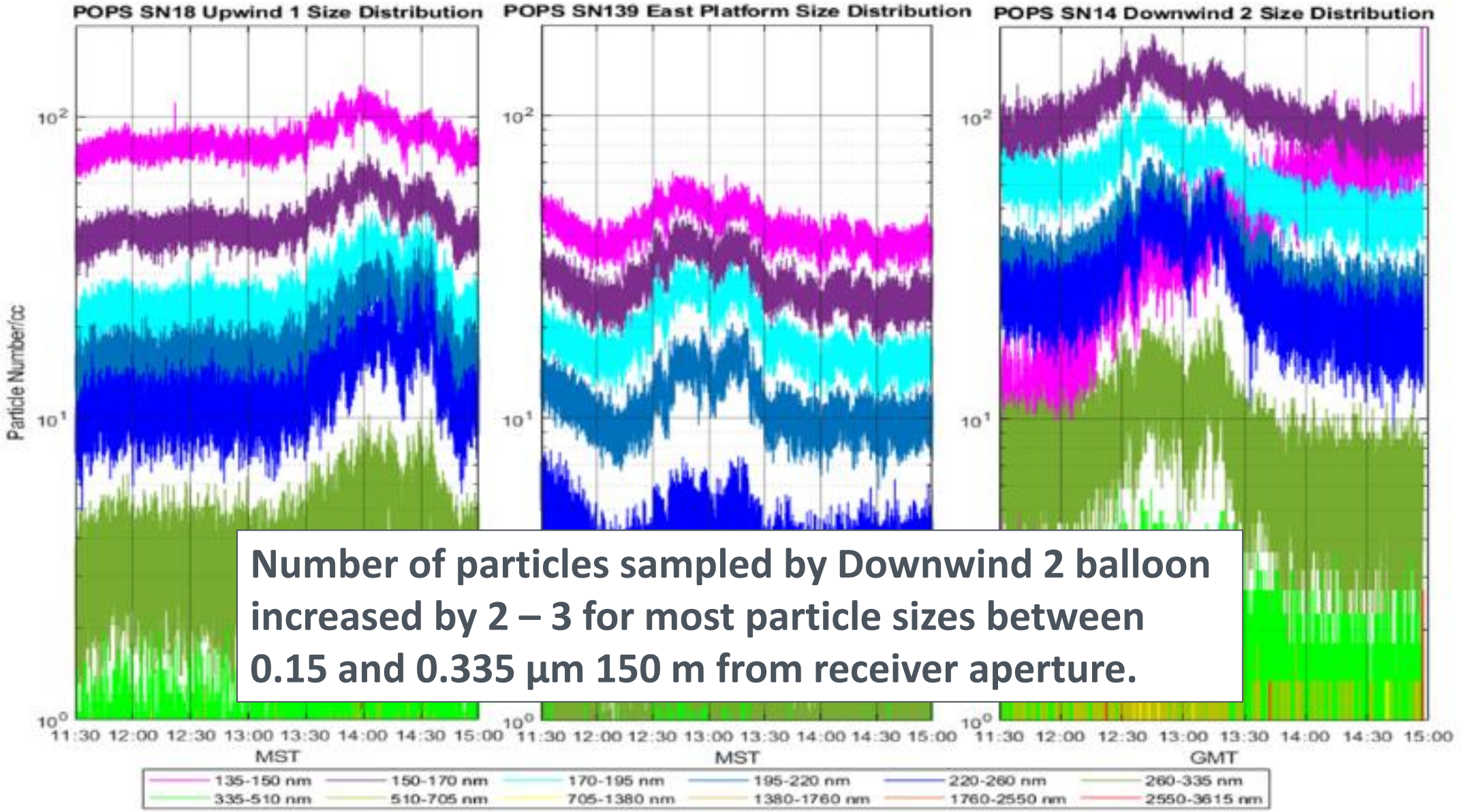

Number of particles sampled by Downwind 2 balloon increased by 2 – 3 for most particle sizes between 0.15 and 0.335 µm 150 m from receiver aperture.

Far-Field Sampling: Upwind – Downwind 1

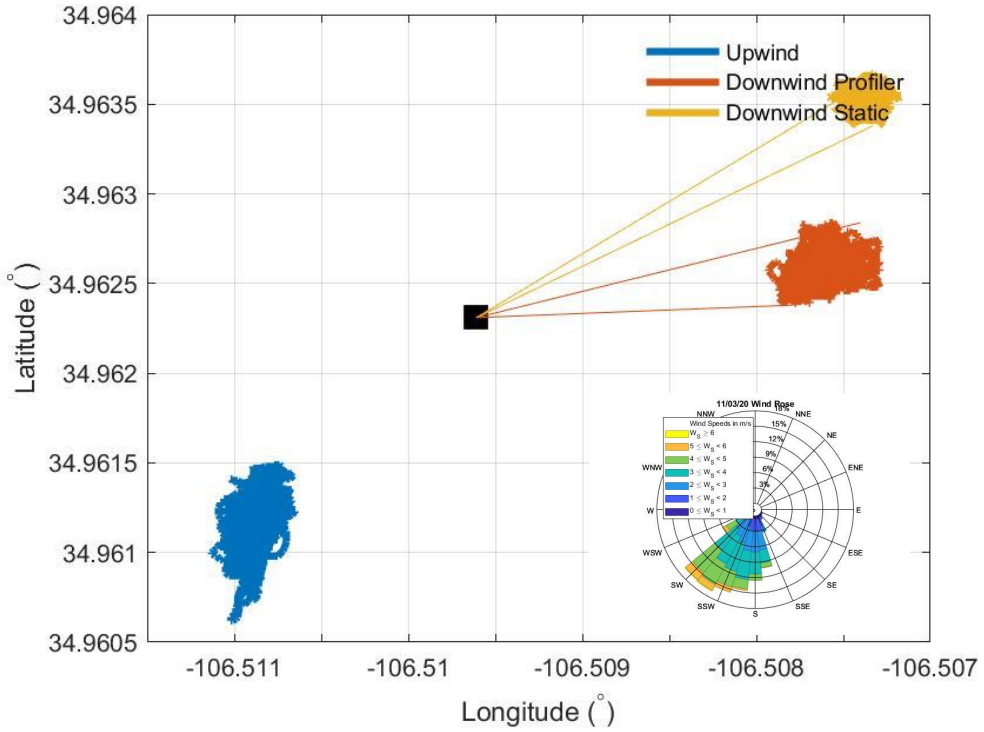

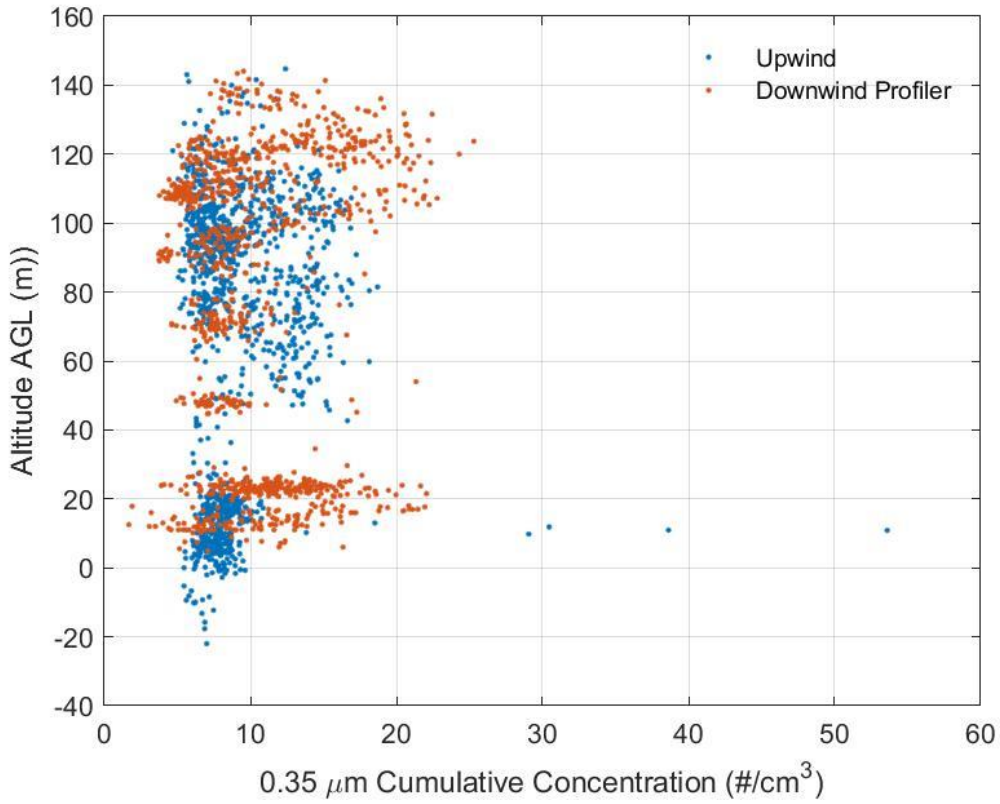

Downwind 1 balloon (profiler) saw minimal increase in particles (not exactly aligned with wind).

Far-Field Sampling – Video of Downwind 1 Profiler, Nov. 3, 2020

Far-Field Sampling Next Steps

- Utilize existing data for emission factor derivation and comparison to regulatory standards (OSHA & NAAQS)
- Second Far-Field Study planned for February 2020
  - Lessons Learned
  - Climatology
  - Locations for Deployment

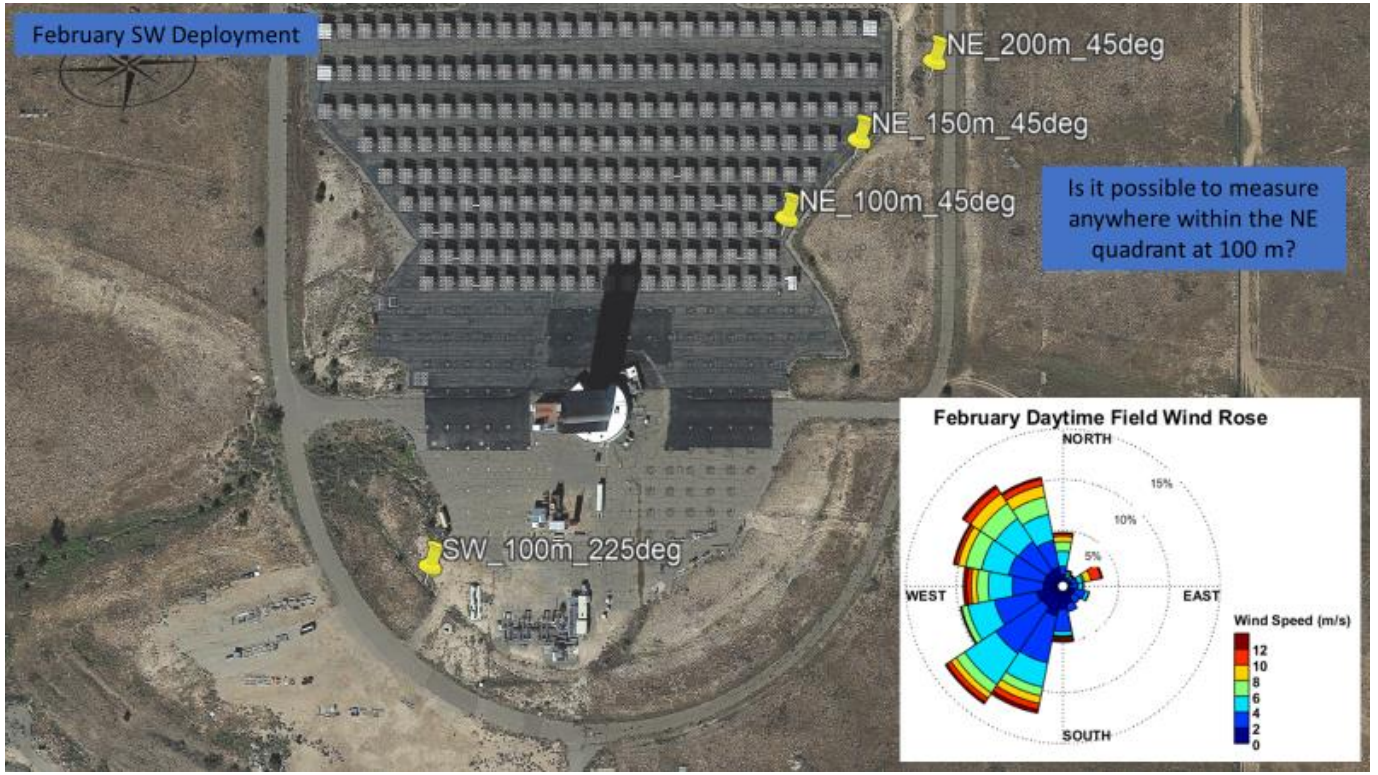

Next Steps

- **Task 1 – Particle Imaging**
  - Now – 5/31/21:
    - Complete on-sun testing and post-process data
    - Complete bench-scale testing using different particles
    - Finalized ASME ES2021 papers and write sections for final DOE report (due 5/1/21)

- **Task 2 – Particle Sampling**
  - Now – 5/31/21:
    - Complete additional tethered-balloon test together with near-field sampling
    - Finalized ASME ES2021 paper and write sections for final DOE report (due 5/1/21)

Spending Summary

III. Spending Summary by Budget Category							
	Approved Budget per SF-424A				Actual Expenses		
Budget Categories per SF-424a	**BP 1**	**BP 2**	**BP 3**	**Total**	**This Quarter**	**Cumulative**	**%**
a. Personnel	$ 122,522	$ 94,899	$ -	$ 217,421	$ 26,530	$ 147,991	68.07%
b. Fringe Benefits	$ -	$ -	$ -	$ -	$ -	$ -	0.00%
c. Travel	$ -	$ 8,689	$ -	$ 8,689	$ -	$ 400	4.60%
d. Equipment	$ -	$ -	$ -	$ -	$ -	$ -	0.00%
e. Supplies	$ 127,393	$ 17,377	$ -	$ 144,770	$ 6,378	$ 138,946	95.98%
f. Contractual	$ 141,145	$ 102,544	$ -	$ 243,689	$ 50,015	$ 279,955	114.88%
g. Construction	$ -	$ -	$ -	$ -	$ -	$ -	0.00%
h. Other	$ 23,731	$ 15,883	$ -	$ 39,614	$ (545)	$ 19,845	50.09%
i. Total Direct Charges	**$ 414,791**	**$ 239,392**	**$ -**	**$ 654,183**	**$ 82,377**	**$ 587,136**	**89.75%**
j. Indirect Charges	$ 216,705	$ 160,182		**$ 376,887**	$ 40,151	$ 288,218	76.47%
k. Total Charges	**$ 631,496**	**$ 399,574**	**$ -**	**$ 1,031,070**	**$ 122,528**	**$ 875,354**	**84.90%**
DOE Share	$ 631,496	$ 399,574	$ -	$ 1,031,070	$ 122,528	$ 875,354	84.90%
Cost Share	$ 6,375	$ 6,375	$ -	$ 12,750	$ -	$ 12,750.00	100.00%
Cost Share Percentage	1.0%	1.6%	0.0%	1.2%	0.0%	1.5%	1.46%

~$57K remaining as of 1/29/21

Questions?

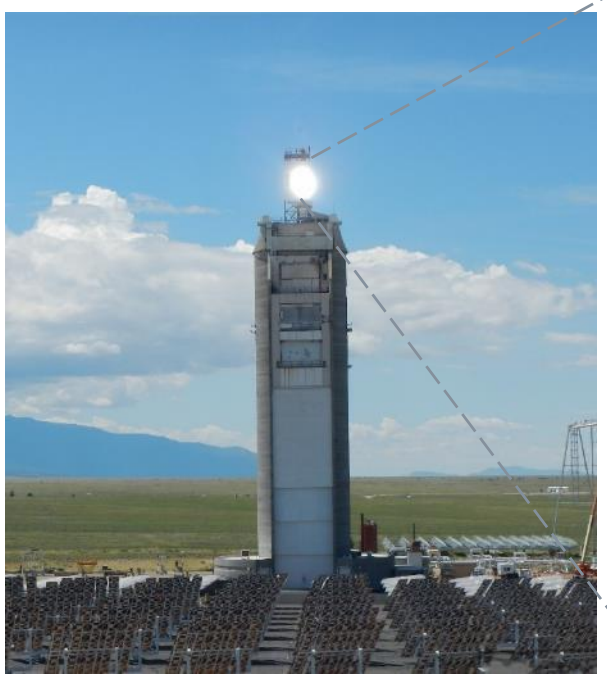

On-sun particle receiver testing at the National Solar Thermal Test Facility at Sandia National Laboratories, Albuquerque, NM

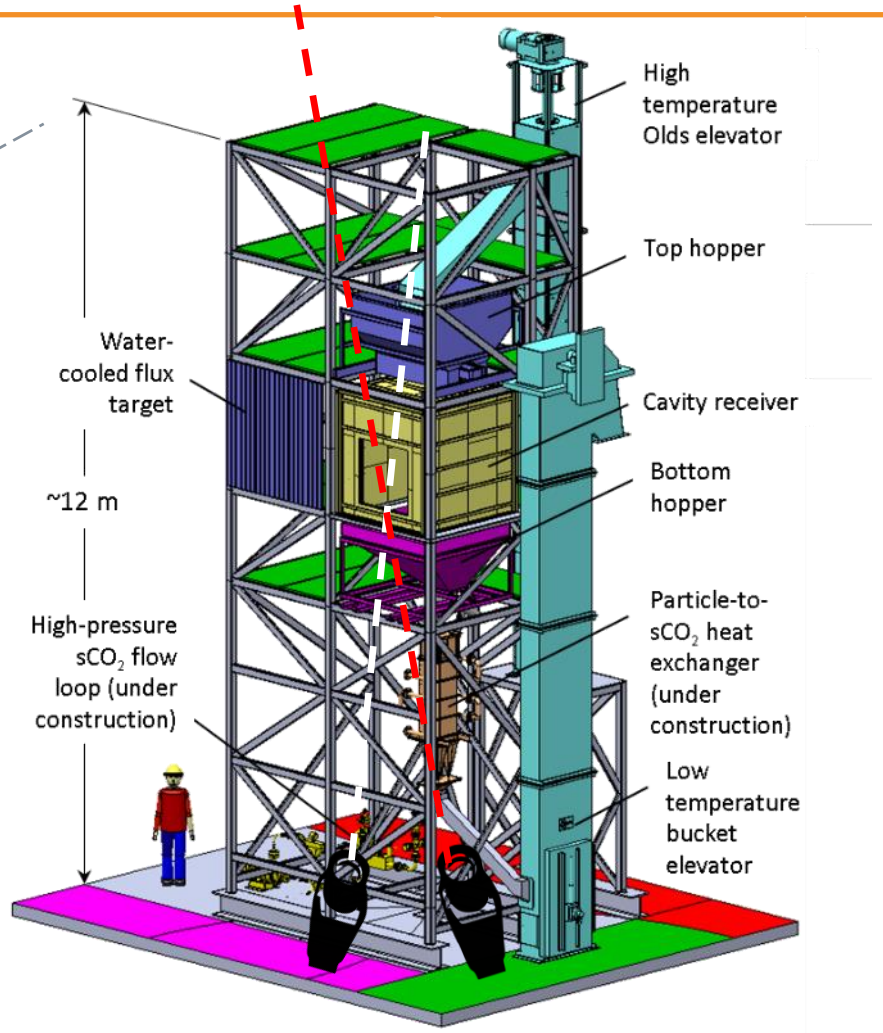

High-Temperature Particle Receiver

Backup Slides